CHAPTER IV

RESULTS AND DISCUSSION

4.1 Physico-Chemical Characterization

In this study, SCP and functionalized SCPs with amino- and mercapto- functional groups were synthesized by co-precipitation method. TEOS was used as silica precursor. Obtained data were combined with adsorption experiment results for study relationships between physico-chemical characteristics (ca. particle size, surface characteristics, hydrophilicity, surface charges, etc.) and heavy metal and ionic dyes adsorption phenomenon.

4.1.1 Particle Size and Surface Area

Particle size was investigated by particle analyzer and scanning electron microscope (SEM). Figure 4.1 showed SEM picture of SCP and functionalized SCP. The average particle size of SCP, AM-SCP, and MP-SCP measured by SEM were 512, 545, and 536 nm, respectively.

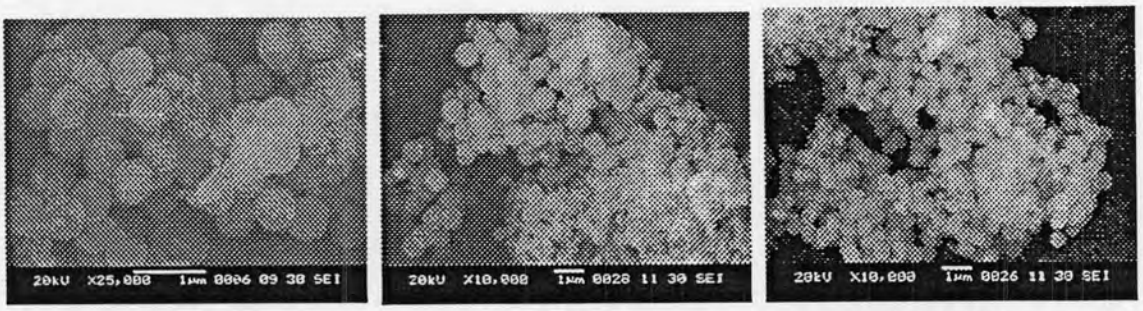

(a.)SCP (b.) AM-SCP (c.) MP-SCP

Figure 4.1 SEM picture of SCP (a.), AM-SCP (b.) and MP-SCP(C.).

The surface areas and average particle size distributions of SCP and functionalized SCP are shown in Table 4.1.

Table 4.1 BET surface area and average particle size of SCP and functionalized SCP.

Adsorbents	BET Surface area (m^2/g)	Average particle Size (nm)	Surface functional groups
SCP	58.01	512	Silanol
AM-SCP	56.84	545	Amino, Silanol
MP-SCP	57.09	536	Mercapto, Silanol

The BET surface area of SCP, AM-SCP, and MP-SCP were found to be 58.01, 56.84, and 57.09 m^2/g, respectively. The specific surface areas of all synthesized SCPs are not different significantly. Hence, surface functional modification by post-grafting method did not affect to the silicate surface structure of SCP.

4.1.2 Surface Functional Groups

Surface functional groups of SCP , AM-SCP, and MP-SCP were investigated by Fourier Transform Infrared (FT-IR) Spectroscopy. It deals with the vibration of chemical bonds in a molecule at various frequencies depending on the elements and types of bonds. In this experiment the FT-IR spectra was used to confirm functional groups on adsorbents surface which loaded during synthesis of functionalized SCPs. The FT-IR spectra of SCP , AM-SCP, and MP-SCP were illustrated in Figure 4.2-4.5.

Figure 4.2-4.5 shows the FT-IR spectra of SCP and functionalized SCPs. All of them exhibit O-H stretching peak at wavenumber of 3400-3500 cm^{-1}. It indicates that they still have silanol groups on surface of materials. Particularly, SCP shows the highest percent transmittance of FT-IR spectra telling that it has more silanol groups than AM-SCP and MP-

SCP. For functionalized SCPs, they express C-H stretching peak at wavenumber of 2930-2965 cm^{-1}. Moreover, AM-SCP exhibits of N-H stretching peak at wavenumber of 3500-3060 cm^{-1} which indicates the presence of NH_2 on surface of SCP. MP-SCP exhibits of S-H stretching peak at wavenumber of 2558 cm^{-1}

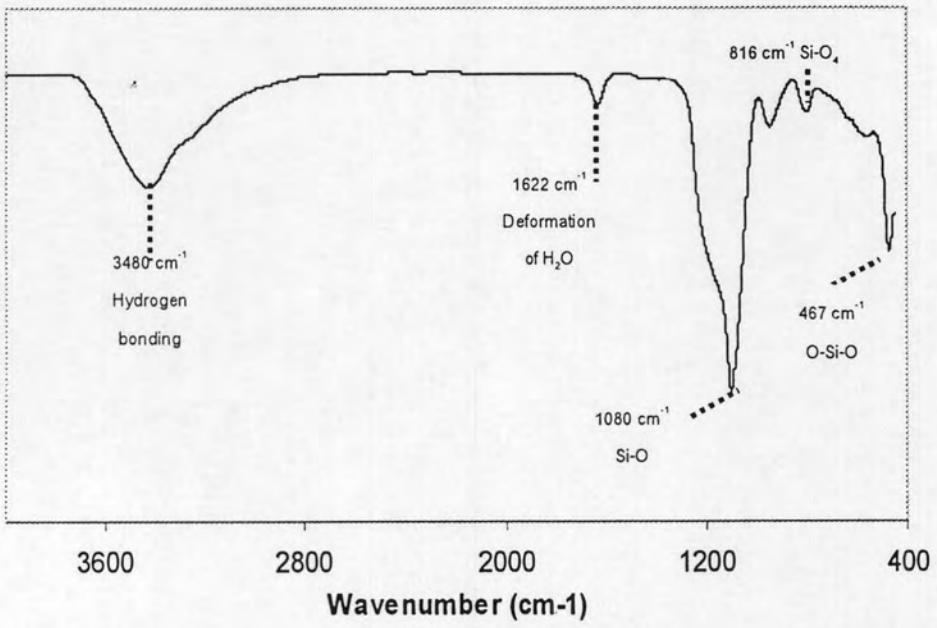

Figure 4.2 FT-IR spectrum of SCP.

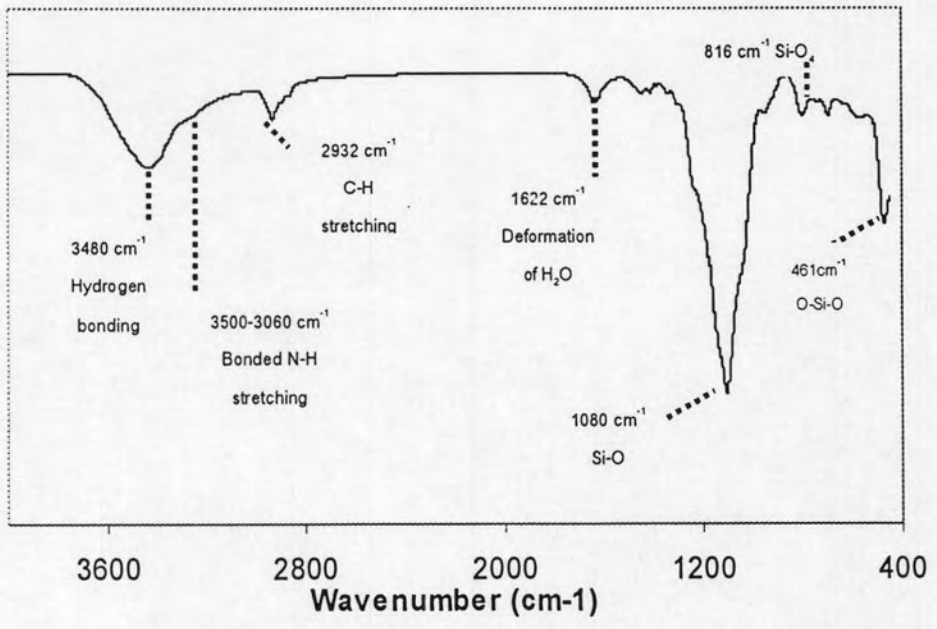

Figure 4.3 FT-IR spectrum of AM-SCP.

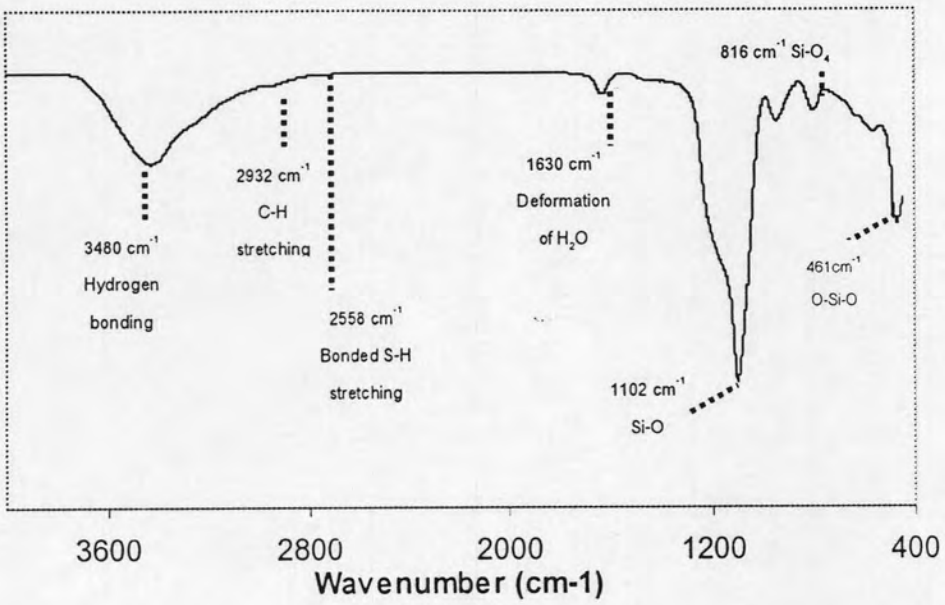

Figure 4.4 FT-IR spectrum of MP-SCP.

4.1.3 Elemental Analysis

In addition to the evidences given by FT-IR spectra, amounts of N and S in AM-SCP and MP-SCP were investigated for confirming the presence of N and S. Autoclave digestion by potassium persulfate ($K_2S_2O_6$) in alkaline condition was conducted for quantitative nitrogen analysis. Inductively Coupled Plasma Atomic Emission Spectroscopy (ICP-AES) technique was applied for S quantification. Pure silicate SCP was also investigated as a blank sample. Amount of N in AM-SCP was quantified as 5.92% (8.214 $x10^{-3}$ mol/g). S in MP-SCP was detected as 1.15% ($5.781x10^{-3}$ mol/g). Obtained results and combination with FT-IR spectra of AM-SCP and MP-SCP can confirmed the presence of amino and mercapto functional groups on the surfaces AM-SCP and MP-SCP, respectively.

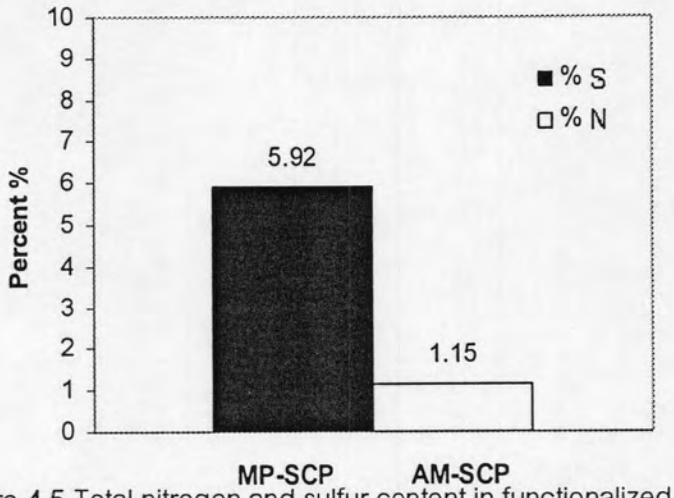

Figure 4.5 Total nitrogen and sulfur content in functionalized SCPs

4.1.5 Surface Charge

Acid/base titration technique was used to determine the surface charge of materials. The ionic strength was fixed at 0.01 M by NaCl solution. After equilibrium, pH of solutions were measured and plotted against surface charges. Surface charges were calculated from the principle of electroneutrality as shown in Equation 4.1.

$$\text{Surface charge (C/g)} = \{[HCl]_{add} - [NaOH]_{add} - [OH^-]\} \times 96500/W \quad (4.1)$$

Where $[HCl]_{add}$ = Concentration of HCl were added (mol/l)

$[NaOH]_{add}$ = Concentration of NaCl were added (mol/l)

$[H^+]$ = Concentration of proton (mol/l) calculated from pH = $-\log[H^+]$

$[OH^-]$ = Concentration of hydroxide ion (mol/l) calculated from pOH = $-\log[OH^-]$ and pOH = 14-pH

96500 = Faraday constant (C/mol)

W = Weight of adsorbent (g/l)

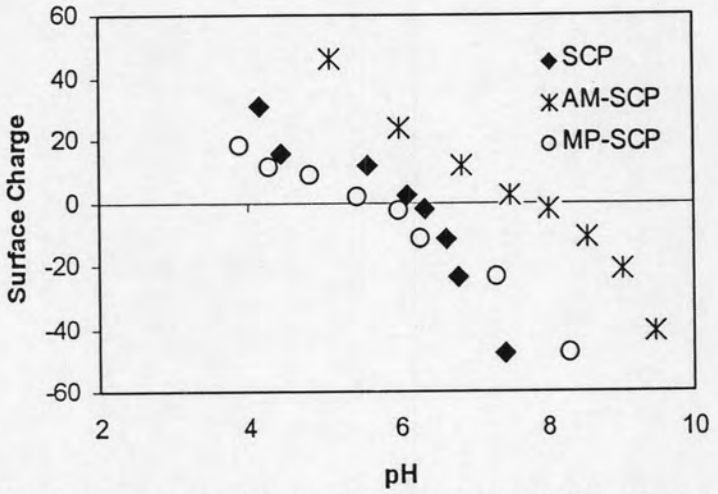

Figure 4.6 Surface charges of SCP , AM-SCP, and MP-SCP as a function of pH.

Figure 4.4 showed the surface charge density of applied adsorbents as function of pH. The pH value that gives zero surface charge is defined as the zero point of charge (pH_{zpc}). pH_{zpc} of all adsorbents was summarized in Table 4.2.

At this pH, the positive charge of cationic surface groups and the negative charge of anionic surface groups are balanced. As shown in Figure 4.4, the surface charge density decrease as the pH increases from acidic region to neutral pH. The silanol groups on the surface of SCPs gain or lose protons, resulting in surface charge variation at different pH as shown in the following equation. At low pH, surface sites of SCPs are protonated and the surfaces become positively charged; whereas at a high pH, the surface hydroxides lose their protons, and the surface becomes negatively charged.

1) Silanol group

$pH < pH_{zpc}$: $\equiv Si - OH + H^+$ $\equiv Si - OH_2^+$

$pH > pH_{zpc}$: $\equiv Si - OH + OH^-$ $\equiv Si - O^- + H_2O$

2) Amino- group

$pH < pH_{zpc}$: $\equiv Si - NH_2 + H^+$ $\equiv Si - NH_3^+$

$pH > pH_{zpc}$: $\equiv Si - NH_2 + OH^-$ $\equiv Si - NH_2OH$

3) Mercapto- group

$pH < pH_{zpc}$: $\equiv Si - SH + H^+$ $\equiv Si - SH_2^+$

$pH > pH_{zpc}$: $\equiv Si - SH + OH^-$ $\equiv Si - SH_2O$

Table 4.2 pH_{ZPC} of SCP , AM-SCP, and MP-SCP.

Adsorbents	pH_{ZPC}
SCP	6.2
AM-SCP	7.8
MP-SCP	5.6

The amino-functional groups presented on SCP gave a higher pH_{zpc} than pristine SCP. Furthermore, surface charge of MP-SCP did not change significantly comparing with SCP.

Table 4.3 Particle size, BET surface area, pH_{zpc}, nitrogen and sulfur content, surface functional groups and hydrophilicity of SCP and functinalized SCPs.

Adsorbents	Particle size (nm)	BET Surface Area (m^2/g)	pH $_{zpc}$	Surface functional groups	Nitrogen content	Sulfur content	Hydrophobicity
SCP	512	58.01	6.2	Silanol	-	-	Hydrophilic
AM-SCP	545	56.84	7.8	Amino	1.15	-	Hydrophilic
MP-SCP	536	57.09	5.6	Mercapto	-	5.92	Hydrophobic

4.2 Adsorption Kinetic

The adsorption rate of heavy metal (Cu(II), Pb(II) and Cd(II)) is shown in Figure 4.7-4.12 at pH 3 and 5. The adsorption rate on SCP, AM-SCP and MP-SCP increases dramatically in first 30 minutes and reached equilibrium stage at about 12 h for Pb(II) and Cd(II). However, adsorption rates of Cu(II) significantly increased in the range of 30 minutes and reached equilibrium stage at around 18 h, slightly slower than Cd(II) and Pb(II). MP-SCP had the highest maximum adsorption capacity of all studied heavy metals. Adsorption kinetic of acid AB and MB at pH 5-9 was shown in Figure 4.13-4.18, adsorption on all adsorbents increases dramatically in first 5 minutes and reached equilibrium stage at about 1 h. MP-SCP and AM-SCP seem to have highest adsorption capacity for MB and AB, respectively.

To analyze the adsorption rate of heavy metals (Cu(II), Pb(II) and Cd(II)) on SCP, AM-SCP and MP-SCP the pseudo-first-order equation of Lagergren and the pseudo-second-order rate were evaluated base on the experimental data. The pseudo-first-order and pseudo-second-order kinetic model are expressed as Eq 4.2 and Eq 4.3 The experimental data were plotted $\ln(q_e-q_t)$ versus time for first-order-rate and plotted t/q_t versus time for second-order rate. The kinetic constants of adsorbents were calculated and listed in Table 4.4-4.15.

$$\ln(q_e - q_t) = \ln q_e - k_1 t \quad (4.2)$$

$$\frac{t}{q_t} = \frac{1}{k_2 q_e^2} + \frac{t}{q_e} \quad (4.3)$$

Where k_1 = Lagergren rate constant (min^{-1})

k_2 = Pseudo-second-order rate constant (g mg^{-1} min^{-1})

q_e = Amounts of heavy metal and ionic dyes sorbed at equilibrium (mg/g)

q_t = Amounts of heavy metal and ionic dyes sorbed at time t (mg/g)

As shown in Fig. 4.7-4.12 and Table 4.4-4.15, it was found that the pseudo-second-order model can be fitted for adsorption of Cu(II), Pb(II), Cd(II), AB and MB onto every adsorbents indicated by the correlation coefficients comparing with pseudo-first-order model. It means the pseudo-second-order rate models could be described adsorption kinetics for Cu(II), Pb(II), Cd(II), AB and MB adsorptions, based on the assumption that the adsorption step may involve chemisorption. Moreover, the experimental q_e values and the calculated q_e obtained from the linear plot in Eq 4.2 were compared as shown in Table 4.4-4.15. The results in Table 4.4-4.15 exhibit very good consistency between that calculated q_e and experimental q_e.

In addition, the initial adsorption rate can also be obtained from this model from Eq 4.3 showed in Table 4.4-4.15.

From calculations, it showed that MP-SCP had the highest initial adsorption rate for heavy metals and MB, but AM-SCP had the highest initial adsorption rate for AB. The calculated data clearly agree with experimental data observed in Figure 4.7-4.18 that initial time, concentration of heavy metals adsorbed onto all adsorbent rapidly decrease, and slowly decrease until equilibrium stage at 12 hr. AB and MB adsorbed onto all adsorbent rapidly decrease, and slowly decrease until equilibrium stage at 1 hr.

In addition, study the effect of pH on the adsorption kinetic for heavy metals and ionic dyes on SCP and functionalized SCP was also shown in Figure 4.7-4.18. The pH of solution was fixed at pH 3 and 5 for heavy metals and at pH 5, 7 and 9 for ionic dyes by phosphate buffer. The result showed that the time to the equilibrium stage for all adsorbent of heavy metals and ionic dyes at different pH had not changed significantly. The initial adsorption rate shown in Table 4.4-4.15 indicated that pH could affect the adsorption rate , however, the relationship between pH and adsorption rates is still unclear.

Table 4.4 Kinetics values calculated for Cu(II) adsorption SCP, AM-SCP and MP-SCP at pH 3

Adsorbent	Pseudo First-order				Pseudo Second-order				
	R^2	k_1 (h^{-1})	Calculated q_e (mg/g)	Experimental q_e (mg/g)	R^2	k_2 (g/mg h)	Calculated q_e (mg/g)	Experimental q_e (mg/g)	h (mg/g h)
SCP	0.7882	0.0083	1.5769	1.712	0.9862	0.3207	1.8726	1.7120	1.1246
AM-SCP	0.9079	0.1658	0.8923	3.611	0.9944	0.0813	3.6692	3.6110	1.0946
MP-SCP	0.7326	0.0276	0.0135	6.431	0.9943	0.0429	6.3642	6.4305	1.7376

Table 4.5 Kinetics values calculated for Pb(II) adsorption onto SCP, AM-SCP and MP-SCP at pH 3

Adsorbent	Pseudo First-order				Pseudo Second-order				
	R^2	k_1 (h^{-1})	Calculated q_e (mg/g)	Experimental q_e (mg/g)	R^2	k_2 (g/mg h)	Calculated q_e (mg/g)	Experimental q_e (mg/g)	h (mg/g h)
SCP	0.6345	0.1244	0.6718	0.9925	0.9914	1.8658	0.8445	0.9925	1.3306
AM-SCP	0.6172	0.2764	0.6002	2.0265	0.9963	0.4264	1.9696	2.0265	1.6542
MP-SCP	0.7883	0.0691	0.6700	3.0556	0.8719	0.0396	3.1821	3.0555	0.4010

Table 4.6 Kinetics values calculated for Cd(II) adsorption onto SCP, AM-SCP and MP-SCP at pH 3

Adsorbent	Pseudo First-order				Pseudo Second-order				
	R^2	k_1 (h^{-1})	Calculated q_e (mg/g)	Experimental q_e (mg/g)	R^2	k_2 (g/mg h)	Calculated q_e (mg/g)	Experimental q_e (mg/g)	h (mg/g h)
SCP	0.5767	0.1382	0.6610	1.3840	0.9987	1.4068	1.3497	1.3840	2.5627
AM-SCP	0.6584	0.0912	6.3771	1.6720	0.9978	0.2688	4.4707	4.3720	5.3725
MP-SCP	0.8766	0.3316	1.9031	1.9825	0.9862	0.3207	1.8726	1.7120	1.1246

Table 4.7 Kinetics values calculated for Cu(II) adsorption SCP, AM-SCP and MP-SCP at pH 5

Adsorbent	Pseudo First-order				Pseudo Second-order				
	R^2	k_1 (h^{-1})	Calculated q_e (mg/g)	Experimental q_e (mg/g)	R^2	k_2 (g/mg h)	Calculated q_e (mg/g)	Experimental q_e (mg/g)	h (mg/g h)
SCP	0.5320	0.0138	0.8965	2.8120	0.9844	0.1250	3.6473	2.8120	1.6629
AM-SCP	0.9285	0.2073	0.3331	7.6110	0.9964	0.0203	7.8373	7.6110	1.2469
MP-SCP	0.9857	0.1520	0.0224	12.4305	0.9457	0.0049	11.6836	12.4305	0.6689

Table 4.8 Kinetics values calculated for Pb(II) adsorption onto SCP, AM-SCP and MP-SCP at pH 5

Adsorbent	Pseudo First-order				Pseudo Second-order				
	R^2	k_1 (h^{-1})	Calculated q_e (mg/g)	Experimental q_e (mg/g)	R^2	k_2 (g/mg h)	Calculated q_e (mg/g)	Experimental q_e (mg/g)	h (mg/g h)
SCP	0.8026	0.1935	2.5639	3.5350	0.9979	0.3989	3.5451	3.5350	5.0134
AM-SCP	0.8199	0.3178	1.5799	4.3765	0.9984	0.2038	4.4890	4.3765	4.1069
MP-SCP	0.9253	0.1658	0.7853	4.0555	0.9560	0.0450	4.1716	4.0555	0.7831

Table 4.9 Kinetics values calculated for Cd(II) adsorption onto SCP, AM-SCP and MP-SCP at pH 5

Adsorbent	Pseudo First-order				Pseudo Second-order				
	R^2	k_1 (h^{-1})	Calculated q_e (mg/g)	Experimental q_e (mg/g)	R^2	k_2 (g/mg h)	Calculated q_e (mg/g)	Experimental q_e (mg/g)	h (mg/g h)
SCP	0.5971	1.2574	1.8097	3.9145	0.9825	0.2280	3.5246	3.9145	2.8324
AM-SCP	0.6668	0.4145	0.7981	2.8720	0.9970	0.3150	2.8803	2.8720	2.6132
MP-SCP	0.7192	0.4007	1.5260	3.8325	0.9975	0.1725	4.0785	3.8325	2.8694

Table 4.10 Kinetics values calculated for AB adsorption onto SCP, AM-SCP and MP-SCP at pH 5

Adsorbent	Pseudo First-order				Pseudo Second-order				
	R^2	k_1 (h^{-1})	Calculated q_e (mg/g)	Experimental q_e (mg/g)	R^2	k_2 (g/mg h)	Calculated q_e (mg/g)	Experimental q_e (mg/g)	h (mg/g h)
SCP	0.5368	0.0967	3.3931	22.2234	0.9981	0.0583	20.7545	14.1667	25.1128
AM-SCP	0.4802	0.2073	6.3241	55.8334	0.9998	0.0038	41.5745	48.0567	149.6835
MP-SCP	0.2749	0.0691	1.0984	6.9433	1.0000	0.0866	17.5527	6.9433	11.7077

Table 4.11 Kinetics values calculated for AB adsorption onto SCP, AM-SCP and MP-SCP at pH 7

Adsorbent	Pseudo First-order				Pseudo Second-order				
	R^2	k_1 (h^{-1})	Calculated q_e (mg/g)	Experimental q_e (mg/g)	R^2	k_2 (g/mg h)	Calculated q_e (mg/g)	Experimental q_e (mg/g)	h (mg/g h)
SCP	0.6804	0.0415	0.2525	18.8900	0.9915	0.0575	15.6162	18.8900	14.0223
AM-SCP	0.4180	1.8931	-	43.9233	0.9986	0.0314	42.3258	43.9233	56.2166
MP-SCP	0.4389	0.0414	-	14.4433	0.9998	0.0778	22.1819	14.4433	38.2807

Table 4.12 Kinetics values calculated for AB adsorption onto SCP, AM-SCP and MP-SCP at pH 9

Adsorbent	Pseudo First-order				Pseudo Second-order				
	R^2	k_1 (h^{-1})	Calculated q_e (mg/g)	Experimental q_e (mg/g)	R^2	k_2 (g/mg h)	Calculated q_e (mg/g)	Experimental q_e (mg/g)	h (mg/g h)
SCP	0.3578	1.6996	1.5764	4.4433	0.9871	0.2288	3.1302	4.4433	2.2418
AM-SCP	0.2407	3.0676	0.5602	11.6667	0.9922	0.0618	13.1152	11.6667	10.6302
MP-SCP	0.7358	0.1658	0.4158	8.8900	0.9999	3.8495	10.4635	8.8900	7.8722

Table 4.13 Kinetics values calculated for MB adsorption onto SCP, AM-SCP and MP-SCP at pH 5

Adsorbent	Pseudo First-order				Pseudo Second-order				
	R^2	k_1 (h^{-1})	Calculated q_e (mg/g)	Experimental q_e (mg/g)	R^2	k_2 (g/mg h)	Calculated q_e (mg/g)	Experimental q_e (mg/g)	h (mg/g h)
SCP	0.4716	0.1935	0.4979	20.4767	0.9994	0.0273	20.3772	15.4767	11.3358
AM-SCP	0.2758	0.2349	0.4587	17.0833	0.9971	0.0499	15.8220	13.8100	12.4918
MP-SCP	0.4092	0.4836	0.9019	23.8100	0.9946	0.0174	24.9376	23.8100	10.8208

Table 4.14 Kinetics values calculated for MB adsorption onto SCP, AM-SCP and MP-SCP at pH 7

Adsorbent	Pseudo First-order				Pseudo Second-order				
	R^2	k_1 (h^{-1})	Calculated q_e (mg/g)	Experimental q_e (mg/g)	R^2	k_2 (g/mg h)	Calculated q_e (mg/g)	Experimental q_e (mg/g)	h (mg/g h)
SCP	0.4482	0.1105	0.3216	29.2867	0.9970	0.0179	27.9396	29.2867	13.9731
AM-SCP	0.3524	0.1244	0.4543	32.8833	0.9981	0.0269	31.8759	32.8833	27.3324
MP-SCP	0.2341	0.0691	0.2211	39.5233	0.9999	0.0493	36.9336	39.5233	67.2495

Table 4.15 Kinetics values calculated for MB adsorption onto SCP, AM-SCP and MP-SCP at pH 9

Adsorbent	Pseudo First-order				Pseudo Second-order				
	R^2	k_1 (h^{-1})	Calculated q_e (mg/g)	Experimental q_e (mg/g)	R^2	k_2 (g/mg h)	Calculated q_e (mg/g)	Experimental q_e (mg/g)	h (mg/g h)
SCP	0.2470	0.5113	0.1389	48.8100	0.9984	0.0043	43.3625	48.8100	8.0853
AM-SCP	0.3181	0.1105	0.8142	12.8567	0.9935	0.1281	12.2963	12.5867	19.3686
MP-SCP	0.1232	0.0415	0.03801	56.9033	0.9994	0.0955	54.7754	56.9033	286.5329

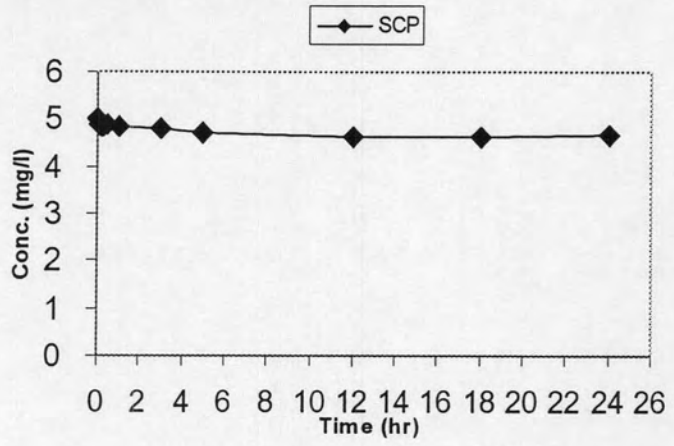

(a) SCP

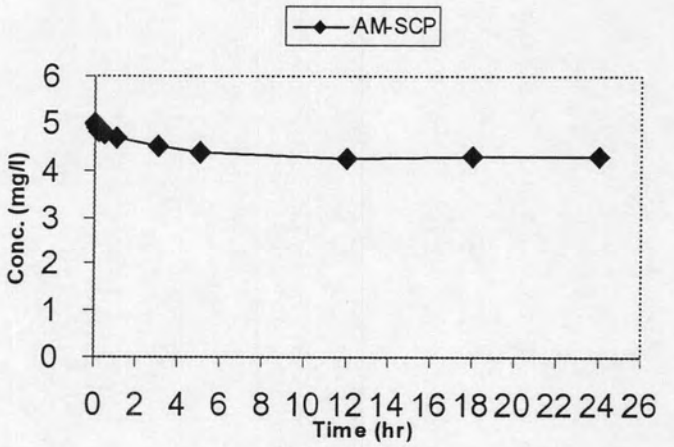

(b) AM-SCP

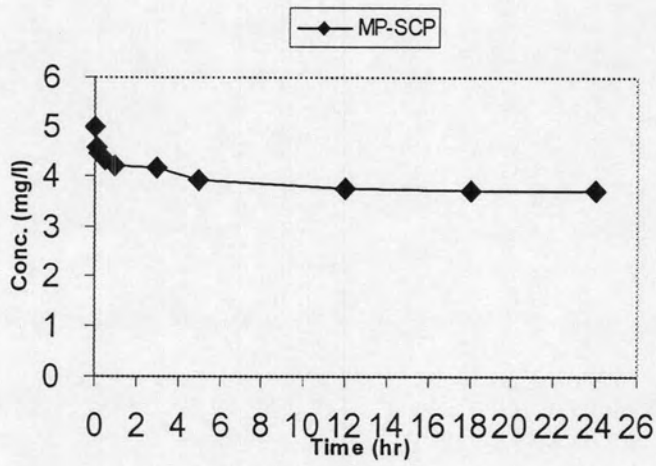

(c) MP-SCP

Figure 4.7 Adsorption kinetic of Cu(II) adsorption onto (a) SCP, (b) AM-SCP and(c) MP-SCP at pH 3, Temperature 25°C and Ionic strength 0.01 M.

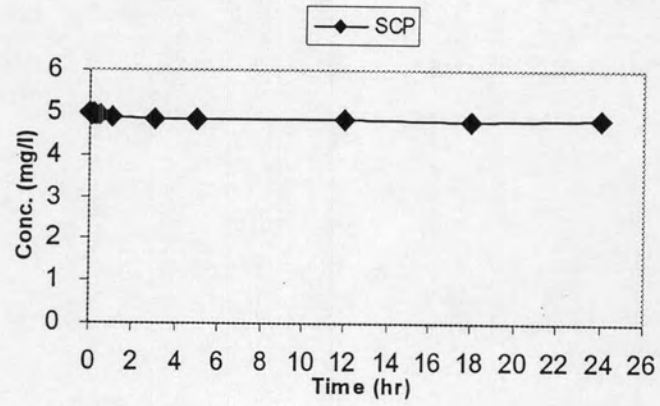

(a) SCP

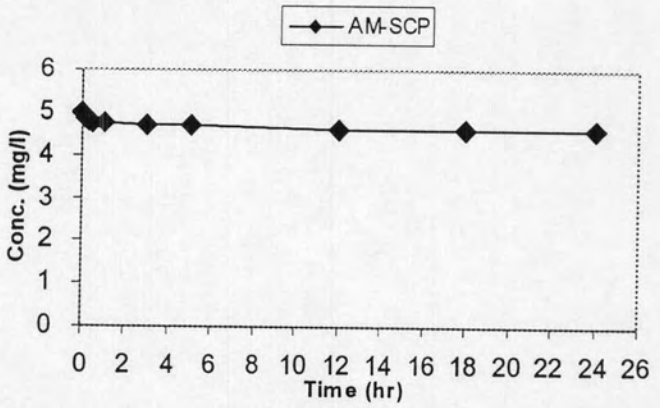

(b) AM-SCP

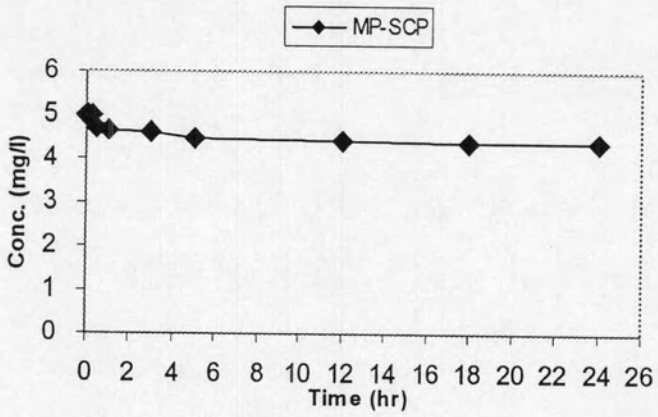

(c) MP-SCP

Figure 4.8 Adsorption kinetic of Pb(II) adsorption onto (a) SCP, (b) AM-SCP and(c) MP-SCP at pH 3, Temperature 25°C and Ionic strength 0.01 M.

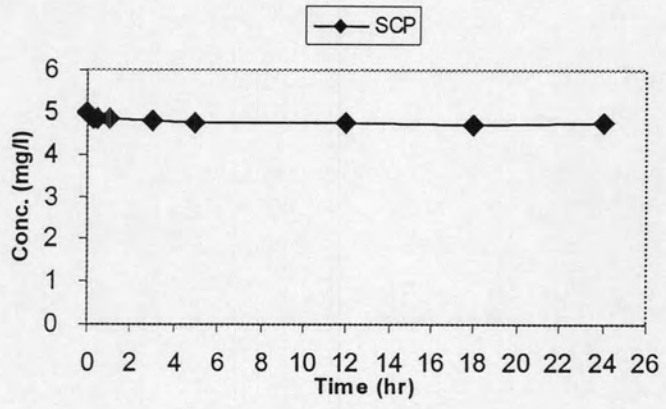

(a) SCP

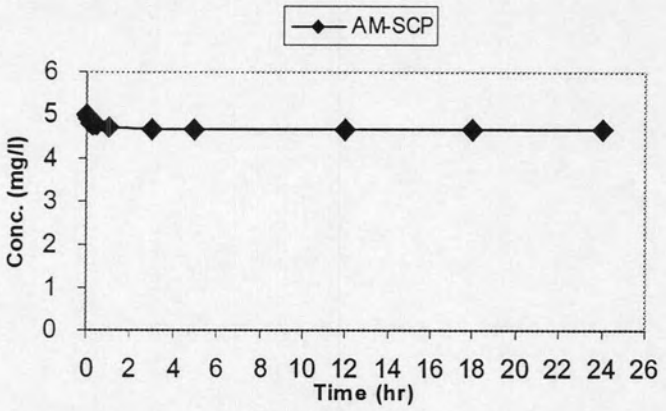

(b) AM-SCP

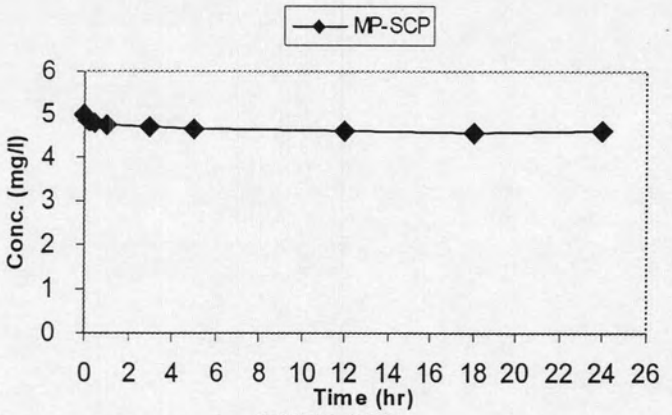

(c) MP-SCP

Figure 4.9 Adsorption kinetic of Cd(II) adsorption onto (a) SCP, (b) AM-SCP and (c) MP-SCP at pH 3, Temperature 25 °C and Ionic strength 0.01 M.

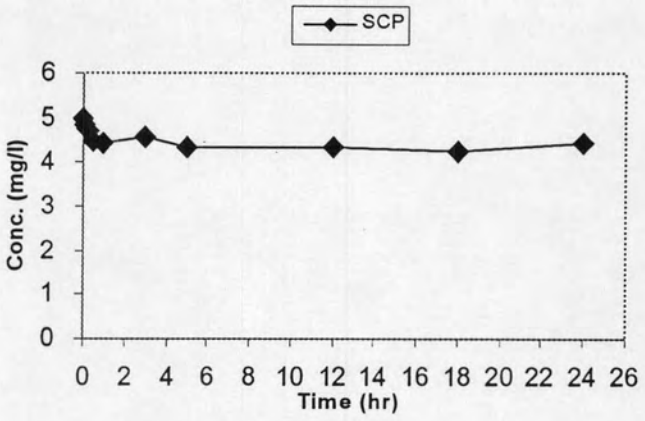

(a) SCP

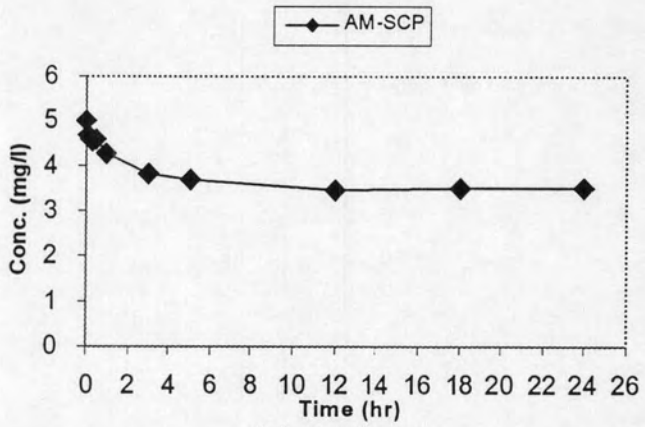

(b) AM-SCP

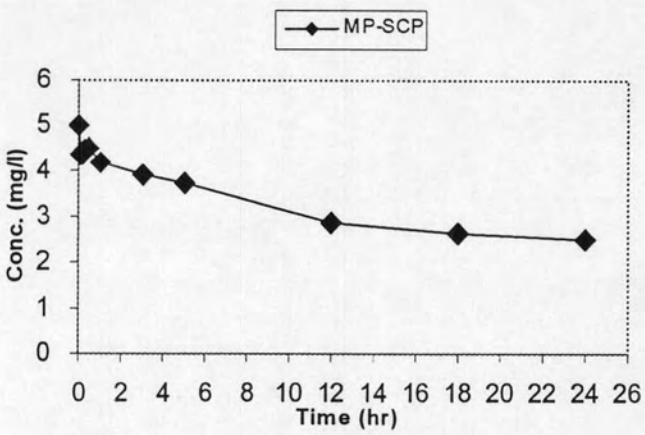

(c) MP-SCP

Figure 4.10 Adsorption kinetic of Cu(II) adsorption onto (a) SCP, (b) AM-SCP and (c) MP-SCP at pH 5, Temperature 25 °C and Ionic strength 0.01 M.

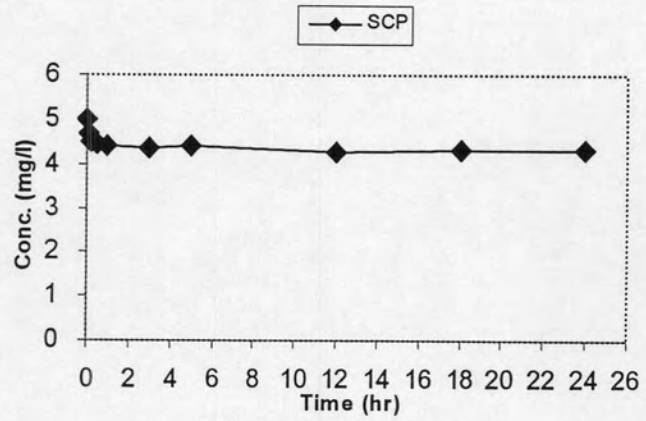

(a) SCP

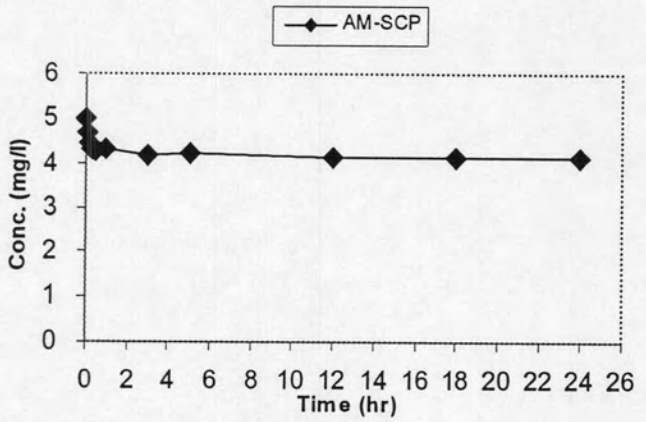

(b) AM-SCP

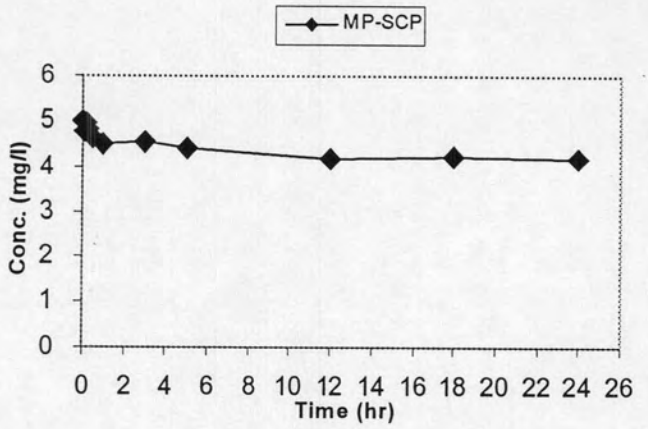

(c) MP-SCP

Figure 4.11 Adsorption kinetic of Pb(II) adsorption onto (a) SCP, (b) AM-SCP and (c) MP-SCP at pH 5, Temperature 25 °C and Ionic strength 0.01 M.

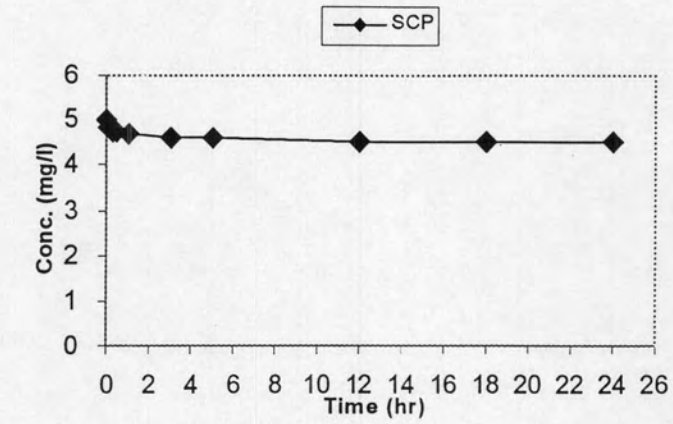

(a) SCP

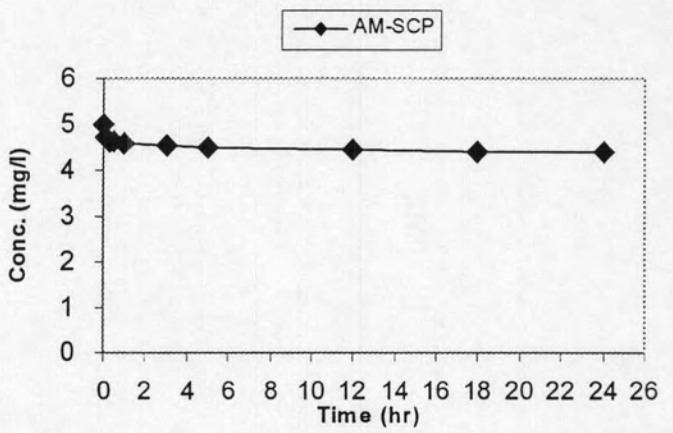

(b) AM-SCP

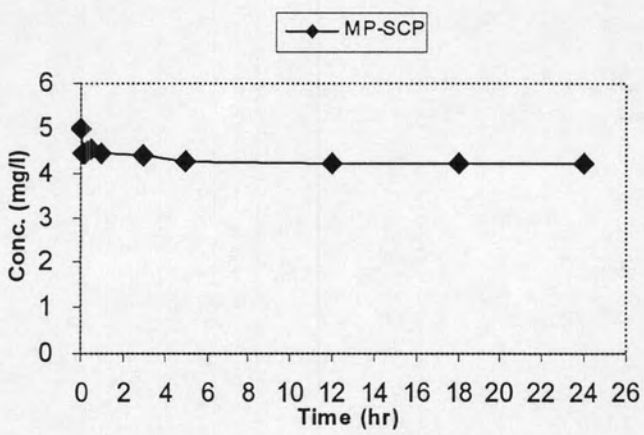

(c) MP-SCP

Figure 4.12 Adsorption kinetic of Cd(II) adsorption onto (a) SCP, (b) AM-SCP and (c) MP-SCP at pH 5, Temperature 25 °C and Ionic strength 0.01 M.

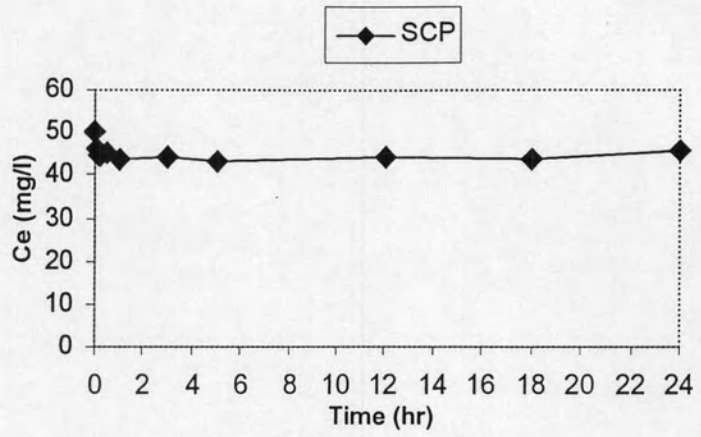

(a) SCP

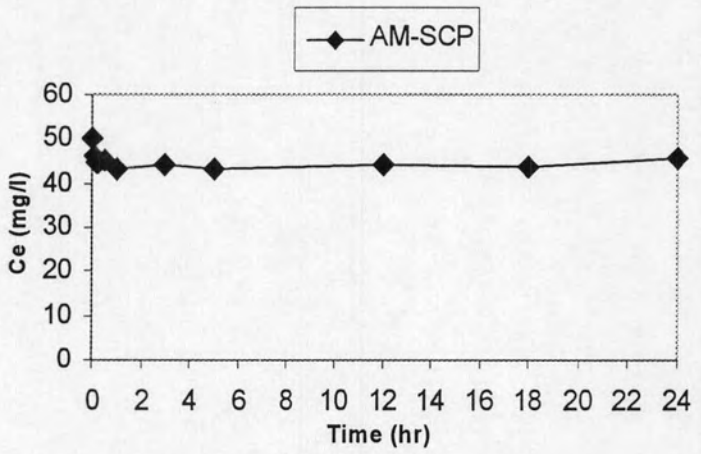

(b) AM-SCP

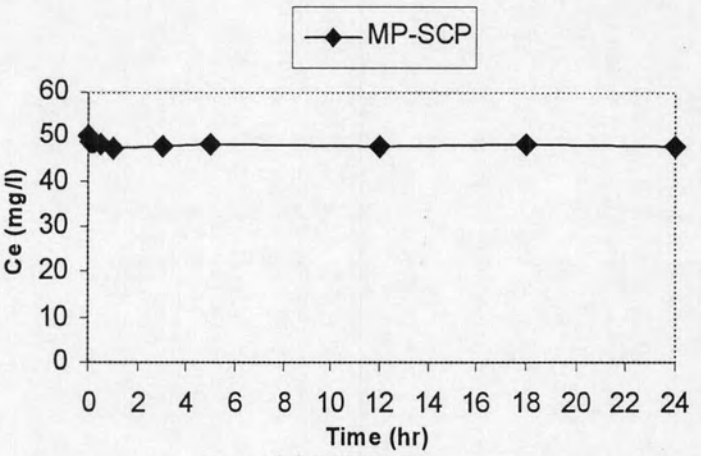

(c) MP-SCP

Figure 4.13 Adsorption kinetic of AB adsorption onto (a) SCP, (b) AM-SCP and (c) MP-SCP at pH 5, Temperature 25 °C and Ionic strength 0.01 M.

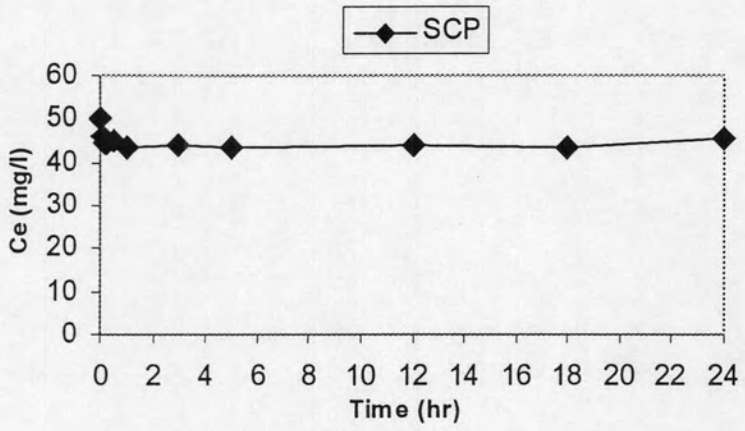

(a) SCP

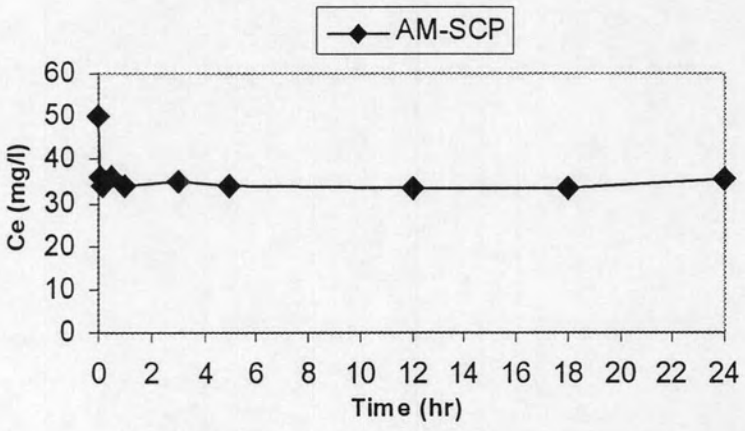

(b) AM-SCP

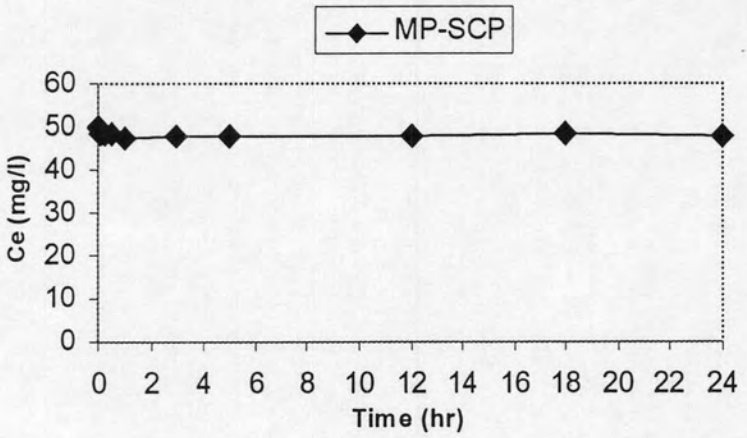

(c) MP-SCP

Figure 4.14 Adsorption kinetic of AB adsorption onto (a) SCP, (b) AM-SCP and (c) MP-SCP at pH 7, Temperature 25 °C and Ionic strength 0.01 M.

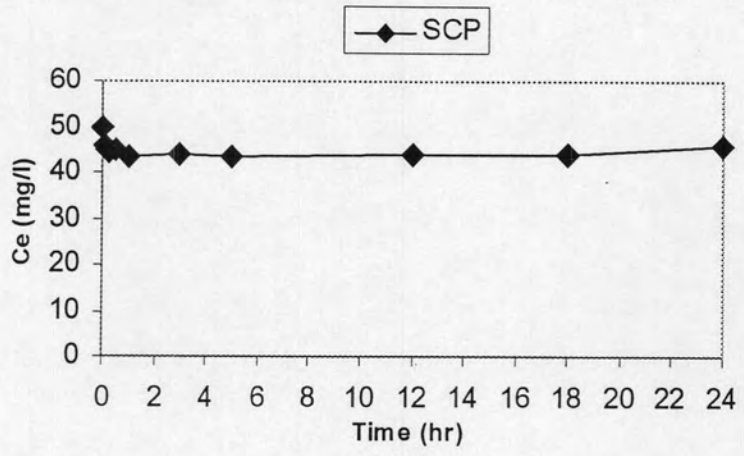

(a) SCP

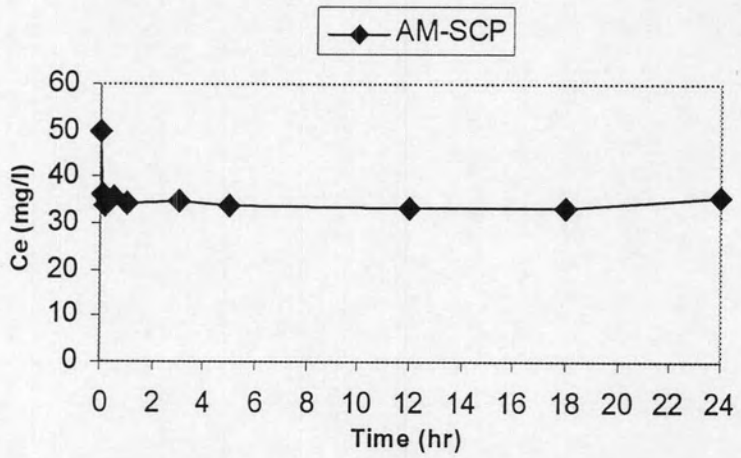

(b) AM-SCP

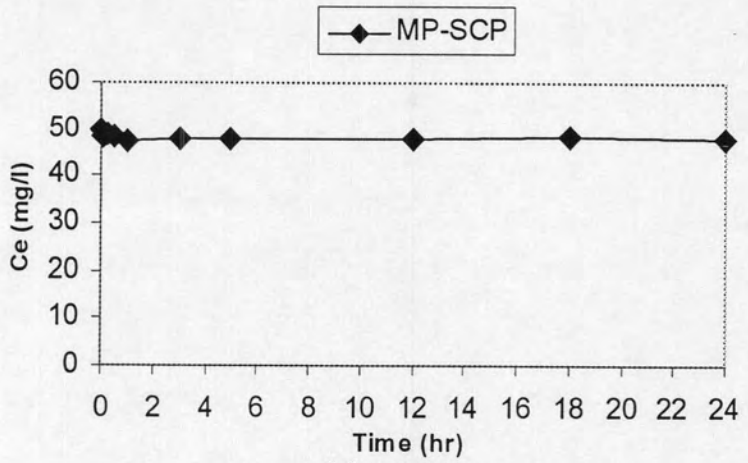

(c) MP-SCP

Figure 4.15 Adsorption kinetic of AB adsorption onto (a) SCP, (b) AM-SCP and (c) MP-SCP at pH 9, Temperature 25 °C and Ionic strength 0.01 M.

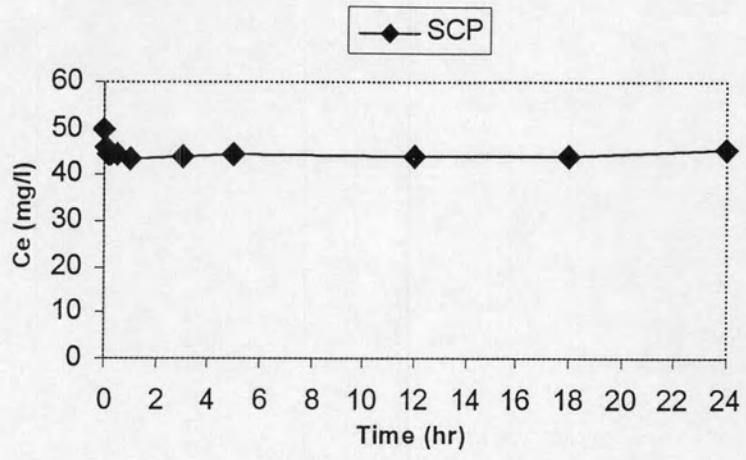

(a) SCP

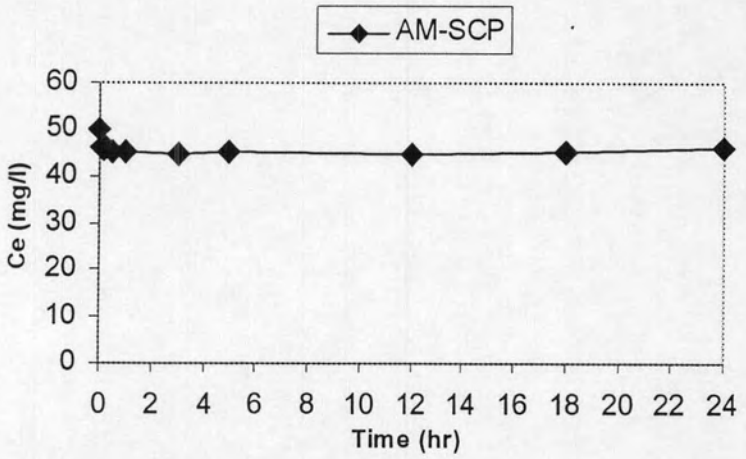

(b) AM-SCP

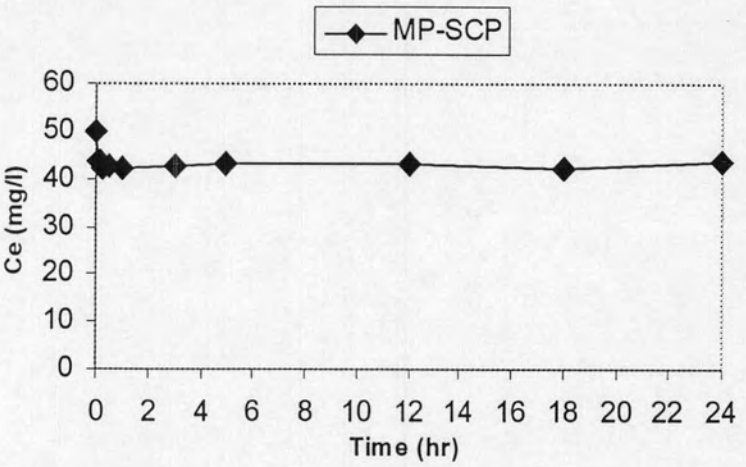

(c) MP-SCP

Figure 4.16 Adsorption kinetic of MB adsorption onto (a) SCP, (b) AM-SCP and (c) MP-SCP at pH 5, Temperature 25 °C and Ionic strength 0.01 M.

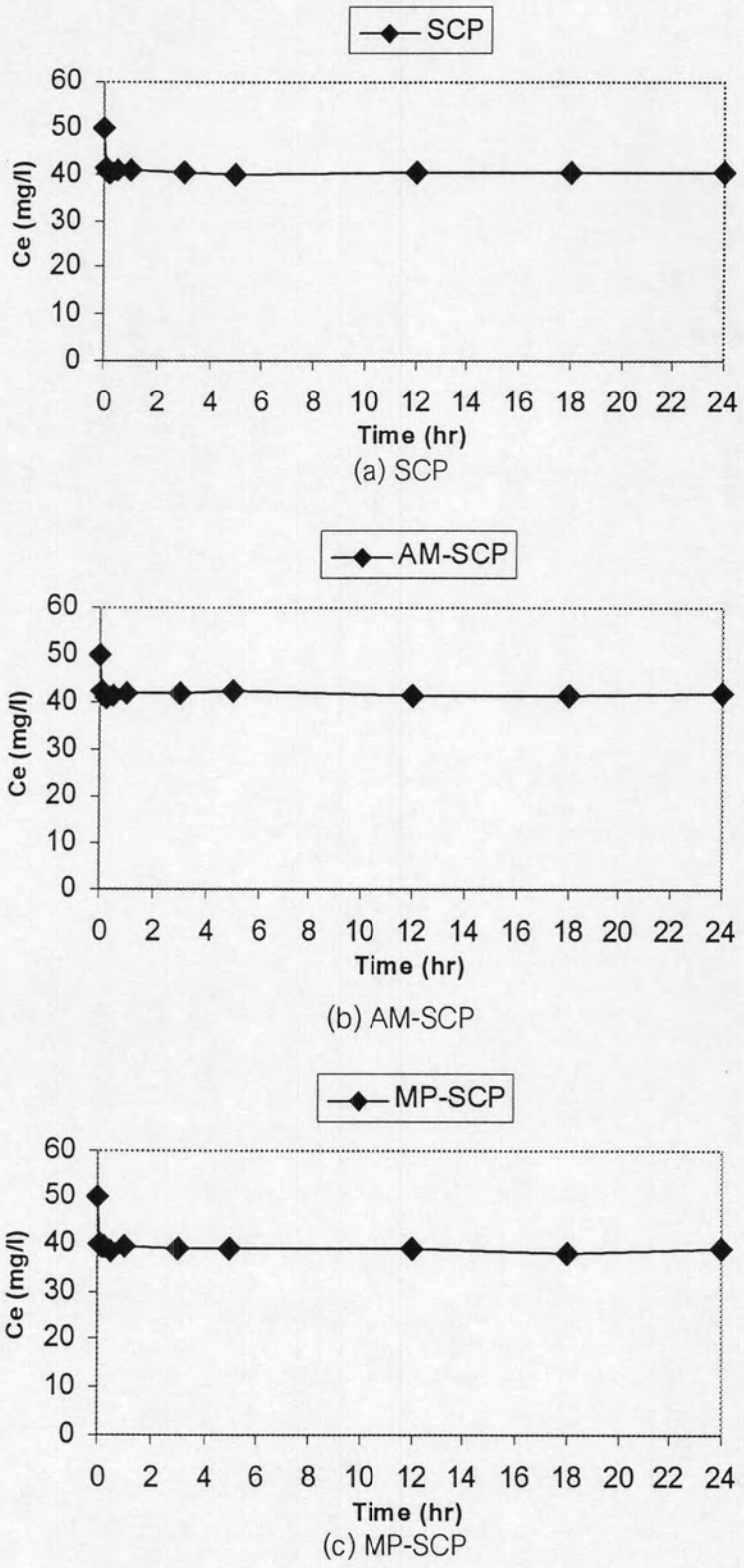

Figure 4.17 Adsorption kinetic of MB adsorption onto (a) SCP, (b) AM-SCP and (c) MP-SCP at pH 7, Temperature 25 °C and Ionic strength 0.01 M.

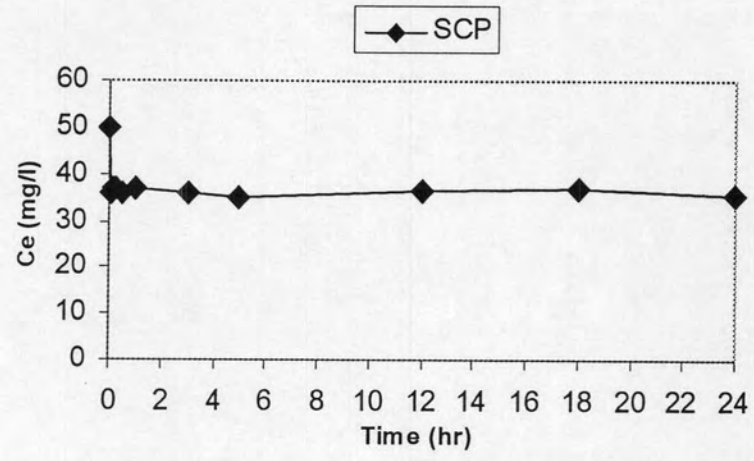

(a) SCP

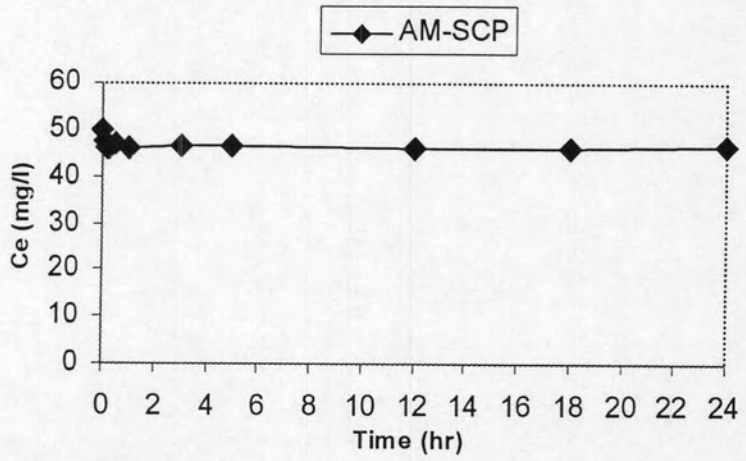

(b) AM-SCP

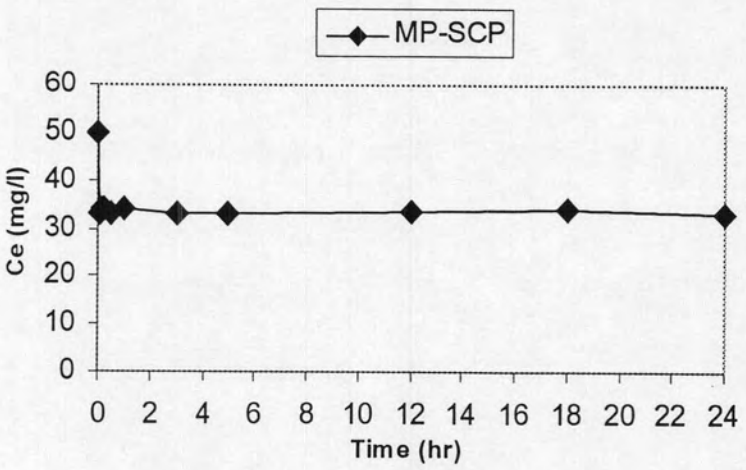

(c) MP-SCP

Figure 4.18 Adsorption kinetic of MB adsorption onto (a) SCP, (b) AM-SCP and (c) MP-SCP at pH 9, Temperature 25 °C and Ionic strength 0.01 M.

4.3 Adsorption Isotherm

Adsorption isotherm was applied to evaluate the sorption capacity of adsorbents as well as understand the adsorbate-adsorbent interactions. In this study, adsorption mechanisms of heavy metal (Cu(II), Pb(II) and Cd(II)) and ionic dyes (Acid Blue and Methylene Blue) from aqueous solution onto SCP and synthesized SCPs (AM-SCP and MP-SCP) were investigated. Physical characteristics of these materials were investigated and their effects to adsorption mechanisms were discussed. We employed the information from adsorption isotherm together with a theoretical evaluation of the surface properties of adsorbents and adsorbate to elucidate adsorption capacities and mechanisms of SCP, AM-SCP and MP-SCP. Moreover, the experimental results were fitted to Langmuir and Freundlich Equations.

4.3.1 Adsorption isotherm of single solute

4.3.1.1 Heavy metal (Cu(II), Pb(II) and Cd(II))

Ayhan (2008) review, Agricultural by-products and in some cases appropriately modified have shown to have a high capacity for heavy metal adsorption. Toxic heavy metals such as Pb(II), Cd(II), Hg(II), Cu(II), Ni(II), Cr(III), and Cr(VI), as well as some elements from lanthanide and actinides groups have been successfully removed from contaminated industrial and municipal waste waters using different agro waste materials. Biosorption experiments over Cu(II), Cd(II), Pb(II), Cr(III), and Ni(II) demonstrated that biomass Cu(II) adsorption ranged from 8.09 to 45.9 mg/g, while Cd(II) and Cr(VI) adsorption ranged from 0.4 to 10.8 mg/g and from 1.47 to 119 mg/g, respectively , Gardea-Torresdey et al (2004). Adsorption of Cu (II) and Pb (II) by activated carbon from hazelnut husks has been shown to depend significantly on the pH, activated carbon from hazelnut husks dosage, contact time and initial concentration. The activated carbon from hazelnut husks would be useful in treatment of wastewater containing copper and lead metals.

Adsorption isotherm of SCP, AM-SCP and MP-SCP with Cu(II), Pb(II) and Cd(II) were shown in Figure 4.20-4.25. The adsorption isotherms of Cu(II), Pb(II) and Cd(II) can be expressed by either Langmuir and Freundlich equations. The isotherm constants of adsorbents were calculated and listed in Table 4.16-4.17. The experimental results were well fitted to Freundlich equation, comparing with Langmuir equation. We compared the adsorption capacity of the adsorbent for Cu (II) and Pb (II) ions results to those obtained by Mustafa and Oktay (2007) prepared activated carbon was used for removal of copper and lead ions from aqueous solutions by the batch method. The experimental data were analyzed by both Freundlich and Langmuir isotherms. The maximum adsorption capacity of the adsorbent for Cu (II) and Pb (II) ions was calculated from the Langmuir isotherm and found to be 6.645 and 13.05 mg g^{-1}, respectively.

In the case of the solution of bivalent metal, M^{2+} was the main component at pH<6 since hydroxyl species were at very low concentrations. Therefore, the measurements of the adsorption of metal ions were carried out at pH~5 to avoid the effects of hydroxyl species. Chemical reaction between metal ions and surface functional groups were suggested to be an important factor for adsorption of heavy metals as shown in Figure 4.19.

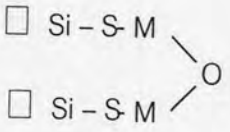

Figure 4.19 Chemical reaction between metal ions and mercapto functional groups on MP-SCP (Lee, et al., 2001).

Figure 4.20-4.25 showed the adsorption isotherm, the order of Cu(II), Pb(II) and Cd(II) affinity was MP-SCP > AM-SCP > SCP. MP-SCP had highest adsorption capacities of Cu(II), Cd(II) and Pb(II) at pH 5 about 13, 6 and 5 mg/g, respectively. Moreover, MP-SCP were higher hydrophobicity comparable with the SCP and AM-SCP, and might be concluded that the hydrophobicity were suggested to be the support factor for adsorption of heavy metals.

We compared the Cu^{2+} adsorption results to those obtained by Leyva-Ramos et al (1997) a concentration at equilibrium of 0.1 mmol/L, the mass adsorbed is 0.036, 0.016 and 0.01mmol/g for Cu^{2+}, Cd^{2+} and Pb^{2+}, respectively, which indicates that the chitosan selectivity for removing heavy metals decreases in the following order: Cu^{2+} $>Cd^{2+}$ $>Pb^{2}$.

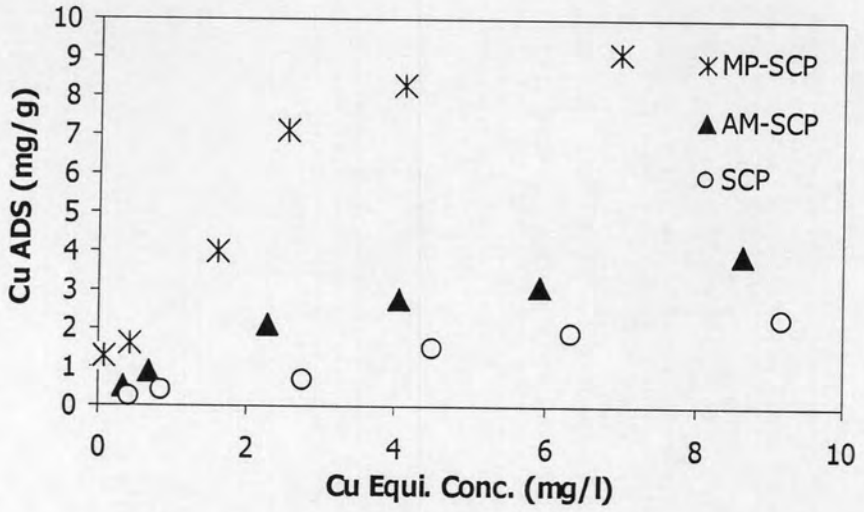

Figure 4.20 Adsorption isotherm of Cu(II) adsorption onto SCP, AM-SCP and MP-SCP at pH of 3, temperature 25 °C and Ionic strength 0.01 M.

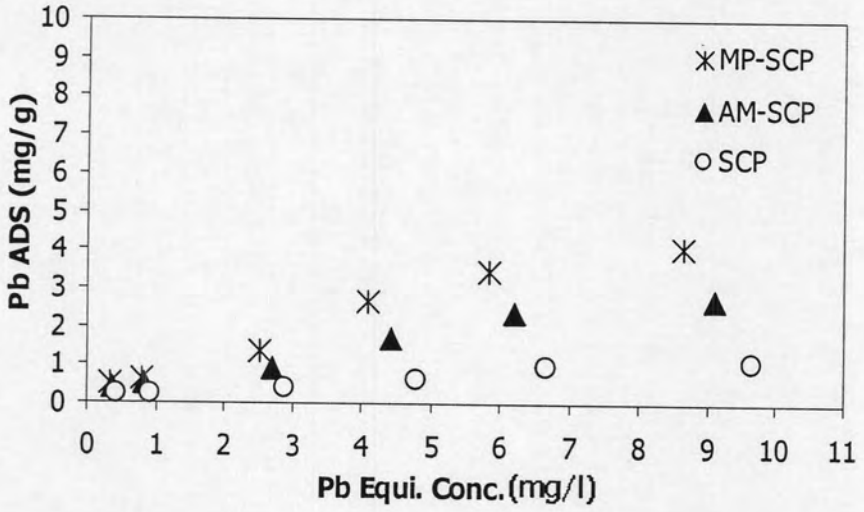

Figure 4.21 Adsorption isotherm of Pb(II) adsorption onto SCP, AM-SCP and MP-SCP at pH 3, Temperature 25 °C and Ionic strength 0.01 M.

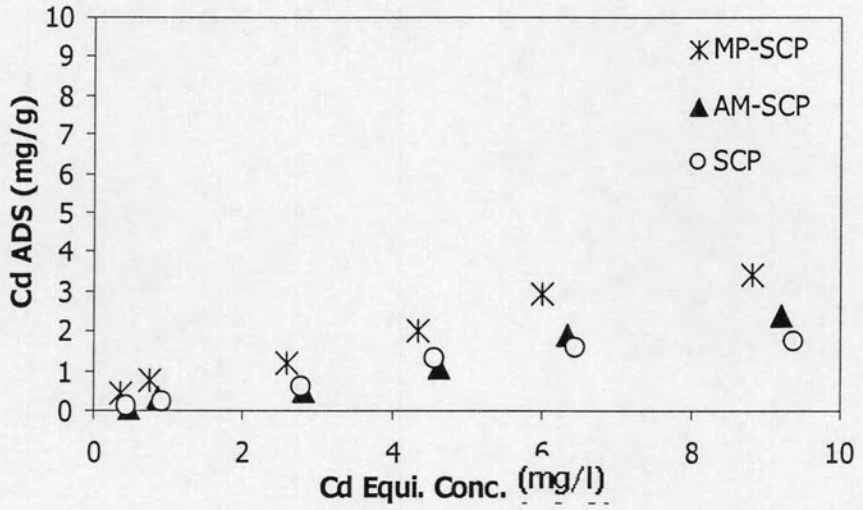

Figure 4.22 Adsorption isotherm of Cd(II) adsorption onto SCP, AM-SCP and MP-SCP at pH 3, Temperature 25 °C and Ionic strength 0.01 M.

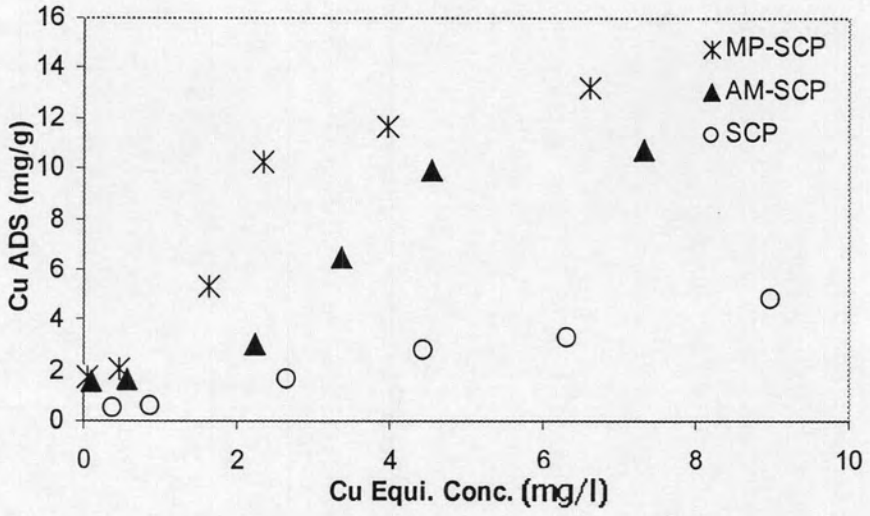

Figure 4.23 Adsorption isotherm of Cu(II) adsorption onto SCP, AM-SCP and MP-SCP at pH 5, Temperature 25 °C and Ionic strength 0.01 M.

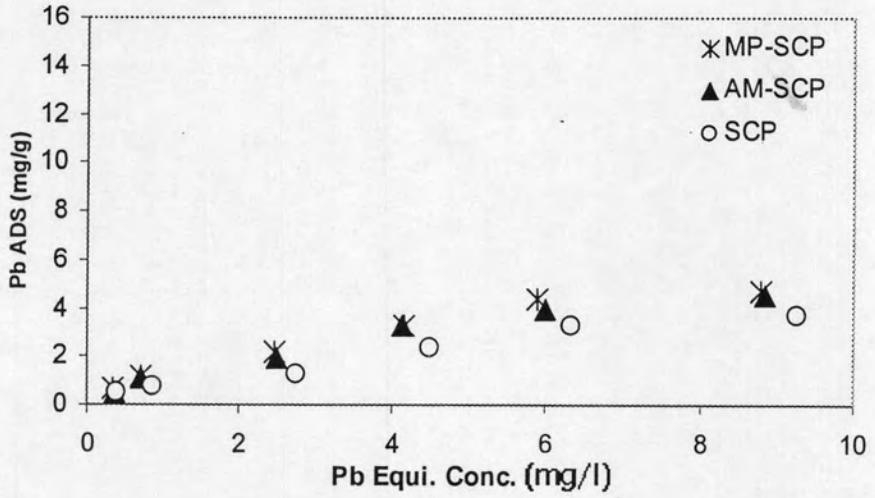

Figure 4.24 Adsorption isotherm of Pb(II) adsorption onto SCP, AM-SCP and MP-SCP at pH 5, Temperature 25 °C and Ionic strength 0.01 M.

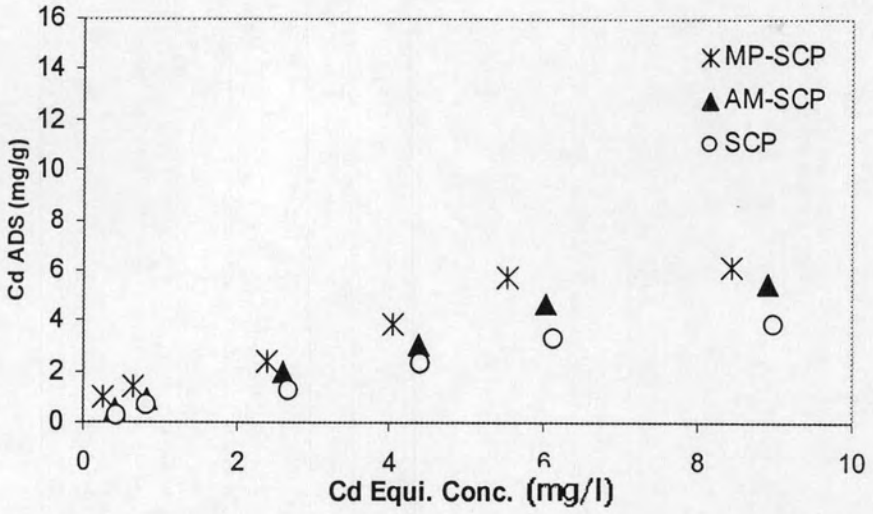

Figure 4.25 Adsorption isotherm of Cd(II) adsorption onto SCP, AM-SCP and MP-SCP at pH 5, Temperature 25 °C and Ionic strength 0.01 M.

4.3.1.2 Ionic dyes (Acid Blue and Methylene Blue)

4.3.1.2.1 Acid Blue 45 (AB)

AB adsorption isotherms of SCP, AM-SCP and MP-SCP were shown in Figure 4.26-4.28. The adsorption isotherms of AB can be expressed by either Langmuir and Freundlich equations. The isotherm constants of adsorbents were calculated and listed in Table 4.19. Electrostatic attraction between negative charge of AB and surface functional groups were suggested to be an important factor for adsorption of AB.

The order of AB affinity was AM-SCP > MP-SCP > SCP. AM-SCP had highest adsorption capacities of AB at pH 5 about 50 mg/g. At pH 5, AM-SCP was exhibits positive charge on surface higher than SCP and MP-SCP, respectively. It was expected that AM-SCP could enhance adsorption capacity for AB by electrostatic attraction with negative charge of AB and positive charge on surface. It was found that MP-SCP had adsorption capacity higher than SCP that it was not onto the electrostatic attraction between negative charge of AB and the surface functional groups. However, van der waals force between hydrophobicity surface on MP-SCP and AB molecule can enhance adsorption capacity of AB on MP-SCP. Moreover, silanol groups on SCP still can adsorb AB that might be caused by hydrogen bonding between nitrogen atom in AB molecule and hydroxyl groups of silanol groups.

Furthermore, the parameters and correlation coefficients of Langmuir and Freundlich isotherm model were calculated by using experimental data through linear regression were listed in Table 4.19. From obtained data, Freundlich isotherm can be fitted to the data with very high correlation coefficients.

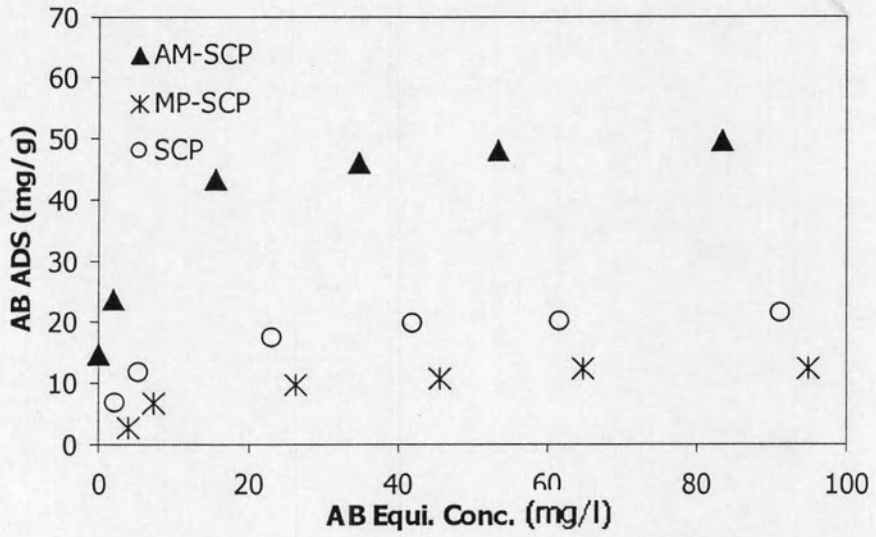

Figure 4.26 Adsorption isotherm of AB adsorption onto SCP, AM-SCP and MP-SCP at pH 5, Temperature 25 °C and Ionic strength 0.01 M.

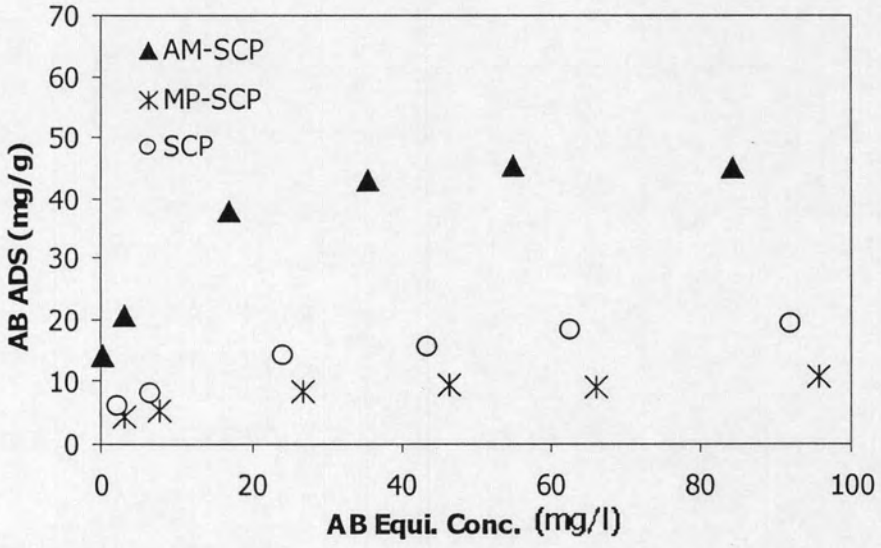

Figure 4.27 Adsorption isotherm of AB adsorption onto SCP, AM-SCP and MP-SCP at pH 7, Temperature 25 °C and Ionic strength 0.01 M.

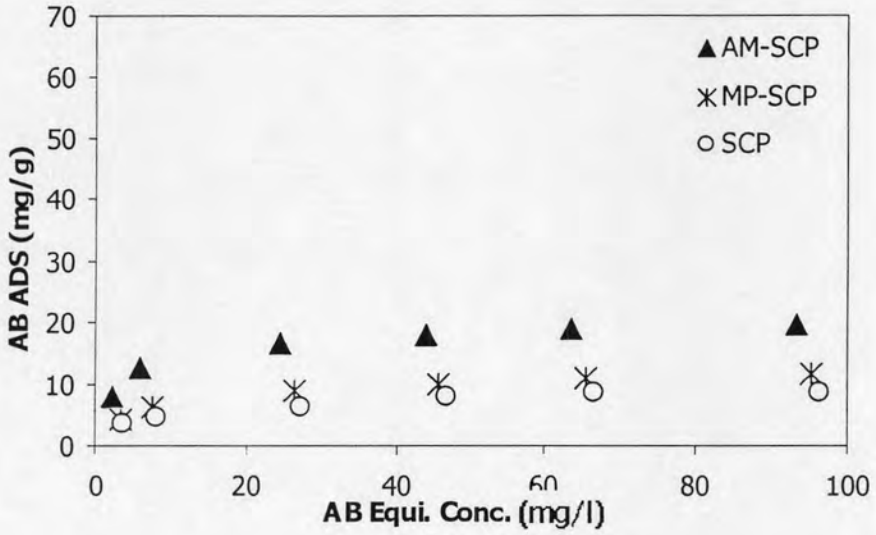

Figure 4.28 Adsorption isotherm of AB adsorption onto SCP, AM-SCP and MP-SCP at pH 9, Temperature 25 °C and Ionic strength 0.01 M.

4.3.1.2.2 Methylene Blue (MB)

MB Adsorption isotherms of SCP, AM-SCP and MP-SCP were shown in Figure 4.29-4.31. The adsorption isotherms of MB can be expressed by either Langmuir and Freundlich equations. The isotherm constants of adsorbents were calculated and listed in Table 4.20. Van der Waals interaction and electrostatic attraction between negative charge of MB and surface functional groups were suggested to be an important factor for adsorption of MB.

The order of MB affinity was MP-SCP > SCP > AM-SCP. MP-SCP had highest adsorption capacity of MB at pH 9 about 90 mg/g. At pH 9, MP-SCP was exhibits negative charge on surface higher than SCP and AM-SCP, respectively. AM-SCP had lowest adsorption capacity of MB. Although it was reported that hydrogen bonding between amino functional group of AM-SCP and molecule of MB can be occurred, however, effect of that hydrogen bonding was suggested to be less than van der Waals interaction due to hydrophobicity of the surface. Moreover, hydrogen bonding

between silanol groups of SCP was supposed to be stronger and can be occurred easier than amino functional groups on AM-SCP (Punyapalakul, et al., 2006). It was expected that MP-SCP could enhance adsorption capacity for MB by electrostatic attraction supporting with positive charge of MB and negative charge on surface. Shaobin et al (2006) used the treated fly ash was tested for adsorption of heavy metal ions and dyes in aqueous solution. The adsorption capacity of methylene blue would increase with pH of the dye solution.

Furthermore, the parameters and correlation coefficients of Langmuir and Freundlich isotherm model were calculated by using experimental data through linear regression were listed in Table 4.20. From obtained data, both of Langmuir and Freundlich isotherm cannot be fitted well for MB adsorption isotherms, however, Freundlich isotherms seem to be fitted better than Langmuir equation, due to higher correlation coefficients.

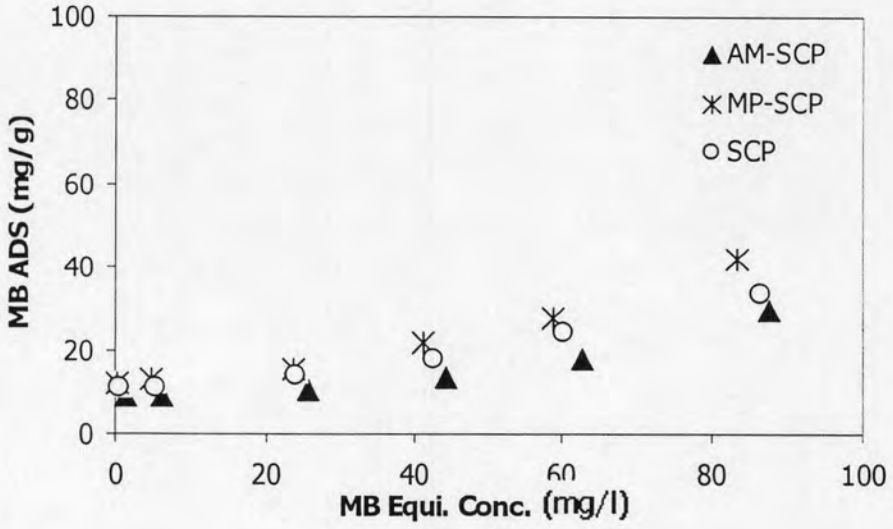

Figure 4.29 Adsorption isotherm of MB adsorption onto SCP, AM-SCP and MP-SCP at pH 5, Temperature 25 °C and Ionic strength 0.01 M.

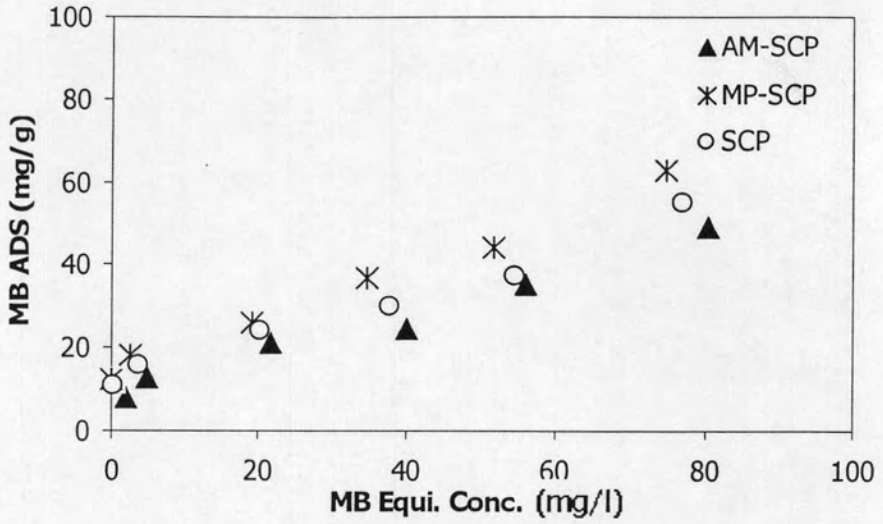

Figure 4.30 Adsorption isotherm of MB adsorption onto SCP, AM-SCP and MP-SCP at pH 7, Temperature 25 °C and Ionic strength 0.01 M.

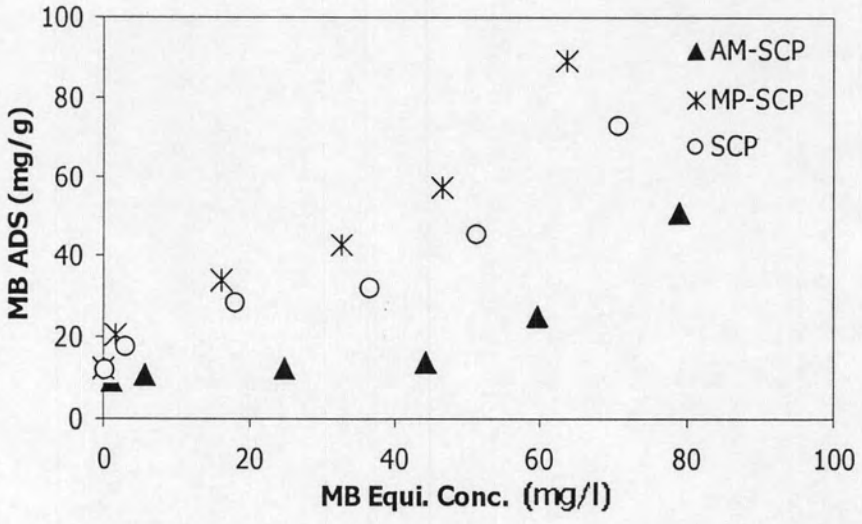

Figure 4.31 Adsorption isotherm of MB adsorption onto SCP, AM-SCP and MP-SCP at pH 9, Temperature 25 °C and Ionic strength 0.01 M.

4.3.2 Effect of pH

To reveal the effect of the electrostatic interaction between adsorbents and ionic dyes, the effects of pH on the adsorption capacities of all adsorbents were investigated by varying pH of solution from 5-9 controlled by phosphate buffer. Furthermore, effect of pH on heavy metals adsorption due to water solubility and effect of hydroxo complex or aqua metal ion were also investigated by varying pH at 3 and 5.

Cadmium can react in solution with carbonates, phosphates, oxalates, arsenates, and cyanides depending on the pH of the solution, this element can also precipitate as hydroxide. Cadmium is mainly found as Cd^{2+} at pH$\leq$8, and from this value up to pH 9 $Cd(OH)^{+}$ ions are formed. At pH> 9 $Cd(OH)_2^{0}$ begins to form; at pH 10.6, 63% of the cadmium present is found as $Cd(OH)_2^{0}$ and the rest is present as $Cd(OH)^{+}$ and $Cd(OH)_3^{-}$; and at pH> 13 the $Cd(OH)_3^{-}$ anions predominate (Stumm, 1996). The effect of pH on the adsorption capacity of Cu(II), Pb(II) and Cd(II) on SCP, AM-SCP and MP-SCP were evaluated within the range of 3 and 5. At pH 5, the adsorption capacities SCP, AM-SCP and MP-SCP of Cu(II), Pb(II) and Cd(II) were higher than at pH 3 that showed in Figure 4.32-4.34. Theoretically, increase of negative charge on surface by increasing pH could enhance adsorption capacity of Cu(II), Pb(II) and Cd(II).

The surface of the adsorbents are expected to be more negatively charged which facilitate the adsorption of the positively charged Cu(II), Pb(II) and Cd(II). Moreover, effect of positive hydronium ion at low pH on active site or surface functional group might cause the decrease of positive Cu(II), Pb(II) and Cd(II) adsorption capacities. Moreover, at low pH heavy metals can form the hydroxo complex that can increase the positive charge, which might disturb the adsorption on the positive charge surfaces. And, the solubility of heavy metals trend to be lower when the pH was increased, this can make the heavy metals can be removed from the water easier.

From Figure 4.32-4.34 the adsorption capacity of Cu(II) had pattern different to Pb(II) and Cd(II) on SCP, AM-SCP and MP-SCP. Molecular weight of Cu(II), Pb(II) and Cd(II) are 63.5 g/mol, 207.2 g/mol and 112.4 g/mol, respectively, that show Cu(II) have a molecule smaller than Pb(II) and Cd(II), this can make Cu(II) have higher density of charge on molecule than Pb(II) and Cd(II).

The effect of pH on the adsorption capacity of AB on SCP, AM-SCP and MP-SCP were evaluated within pH 5, 7 and 9 were showed Figure 4.35. Acid Blue is an anionic dye, which exhibits negative charged ions in aqueous solution. The adsorption capacities of AB on all of adsorbents at pH 5 and 7 were higher than at pH 9, especially for SCP and AM-SCP. It can be explained by the electrostatic interaction of negative charged of AB with the positive charged of adsorbents surface. However, it was found that adsorption capacities of AB on MP-SCP did not affect by pH changing significantly, this might be supposed that adsorption mechanism of AB on mercapto functional groups should be only van der Waals interaction.

The effect of pH on the adsorption capacity of MB on SCP, AM-SCP and MP-SCP were evaluated within pH 5, 7 and 9 were showed Figure 4.36. Methylene Blue is an cationic dye, which exhibits positive charged ions in aqueous solution. The adsorption capacities of MB on all of adsorbents at pH 9 higher than at pH 7 and pH 5. It was explained by the electrostatic interaction of positive charged of MB with the negative charged of adsorbents surface. The electrostatic interaction force of the dye with the adsorbents surface is likely to be raised when the pH increases. At pH 5 the surfaces tend to be protonated and have positive charge, which can decrease the MB adsorption capacity. However, effects of electrostatic interaction of AM-SCP seem to be less than the others, which can be supposed that hydrogen bonding between amino functional groups and MB molecule play the important role for adsorption mechanism.

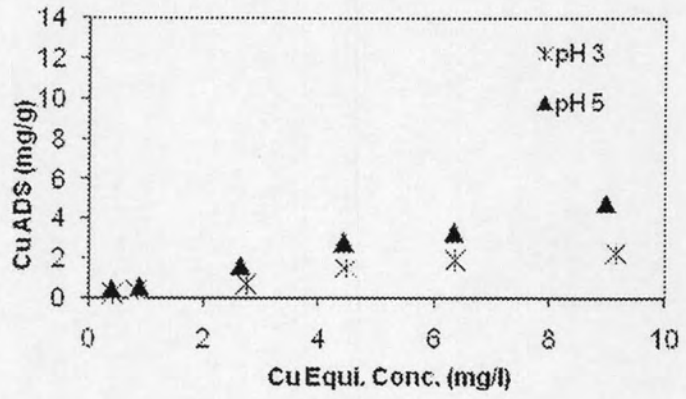

(a) SCP

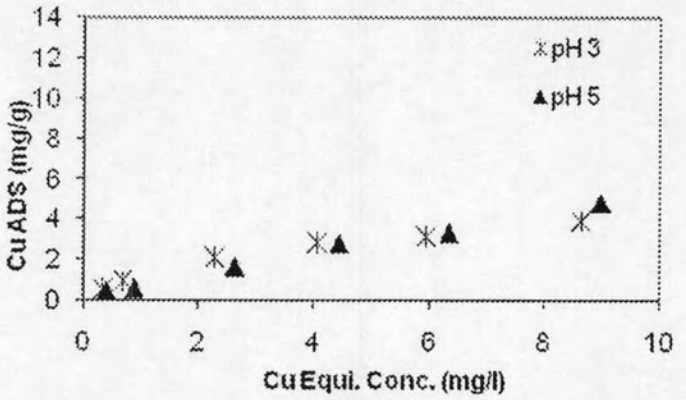

(b) AM-SCP

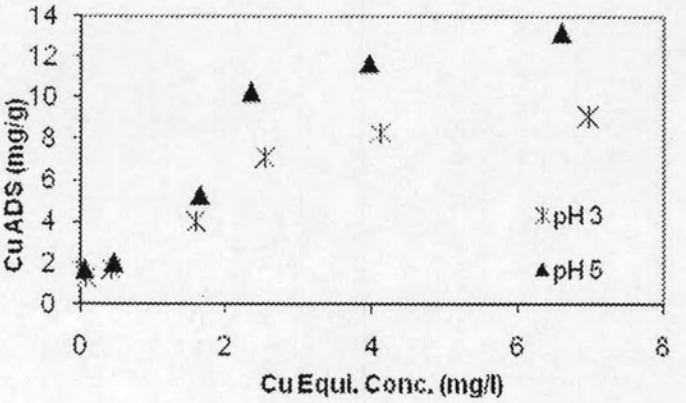

(c) MP-SCP

Figure 4.32 Adsorption isotherm of Cu(II) adsorption onto (a) SCP, (b) AM-SCP and (c) MP-SCP at different pH, Temperature 25 °C and Ionic strength 0.01 M.

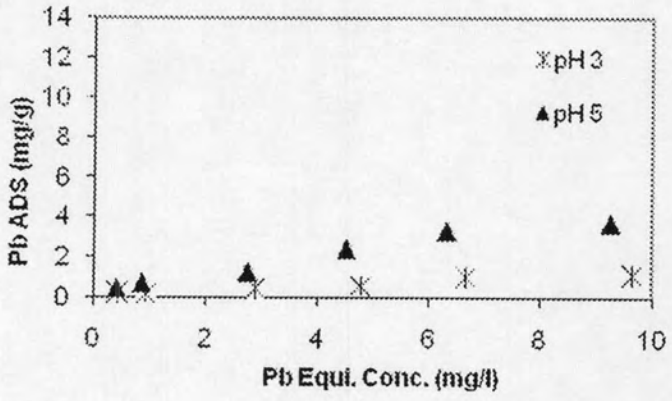

(a) SCP

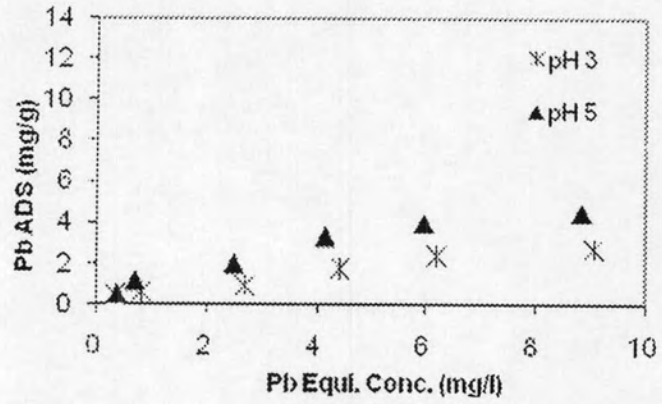

(b) AM-SCP

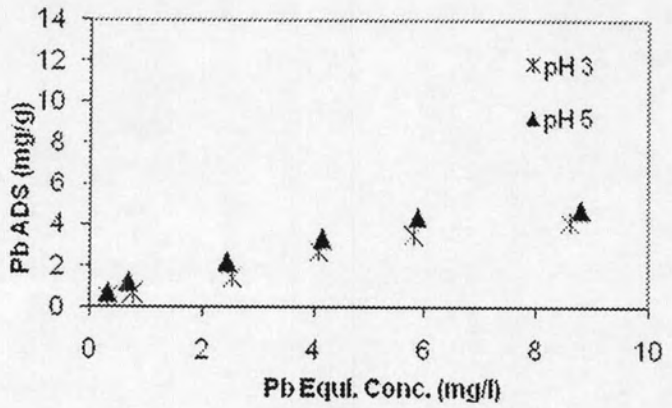

(c) MP-SCP

Figure 4.33 Adsorption isotherm of Pb(II) adsorption onto (a) SCP, (b) AM-SCP and (c) MP-SCP at different pH, Temperature 25 °C and Ionic strength 0.01 M.

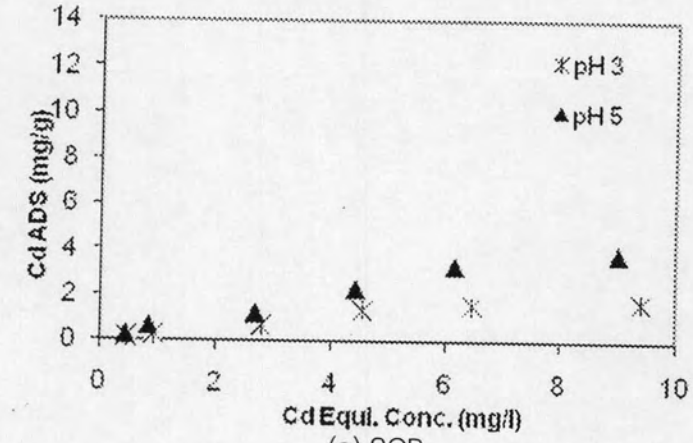

(a) SCP

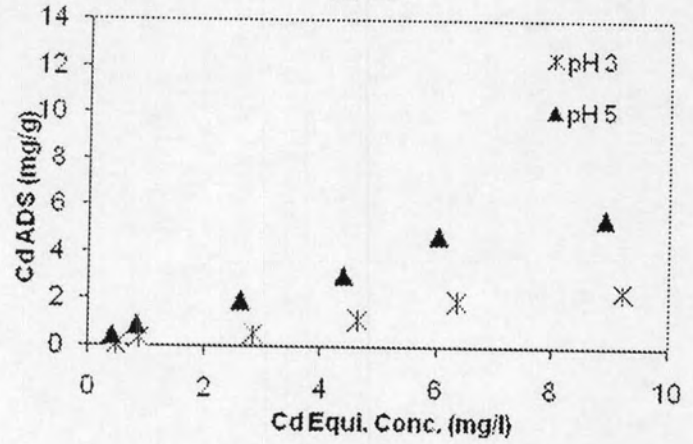

(b) AM-SCP

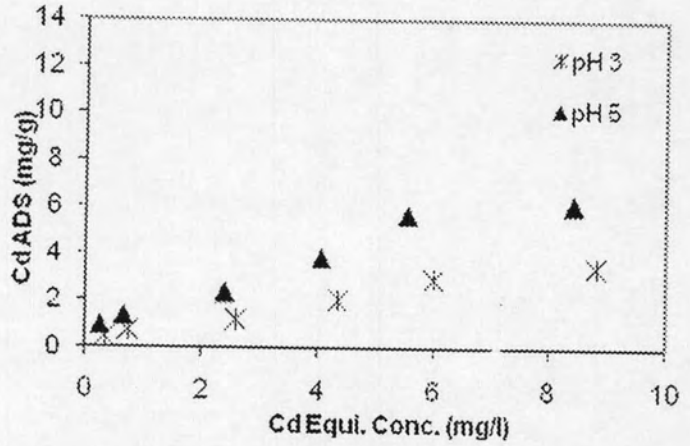

(c) MP-SCP

Figure 4.34 Adsorption isotherm of Cd(II) adsorption onto (a) SCP, (b) AM-SCP and (c) MP-SCP at different pH, Temperature 25 °C and Ionic strength 0.01 M.

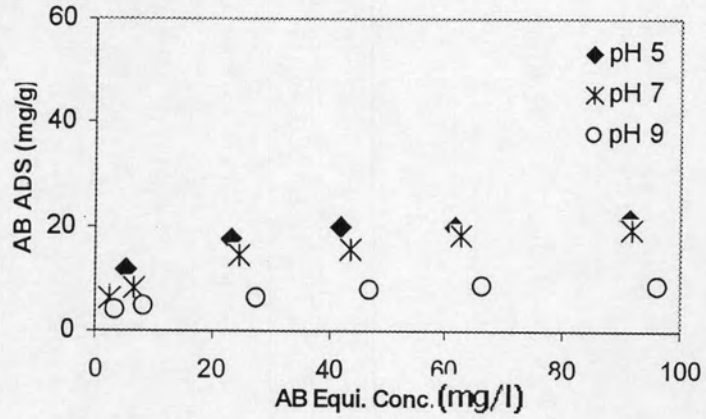

(a) SCP

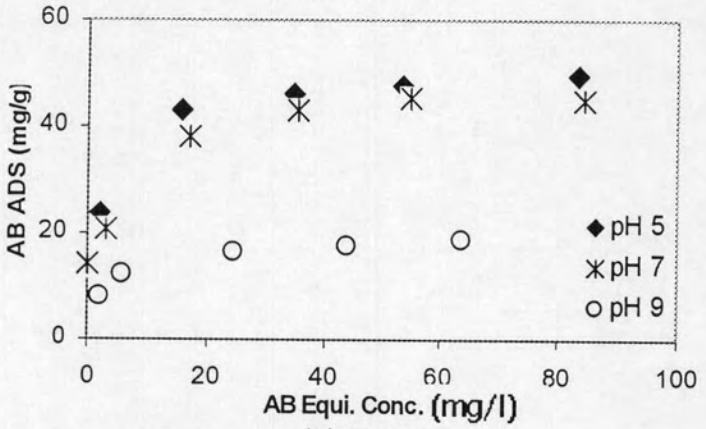

(b) AM-SCP

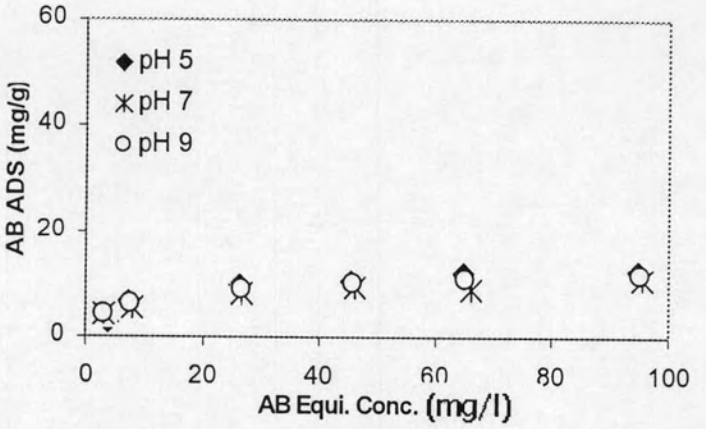

(c) MP-SCP

Figure 4.35 Adsorption isotherm of AB adsorption onto (a) SCP, (b) AM-SCP and (c) MP-SCP at different pH, Temperature 25°C and Ionic strength 0.01 M.

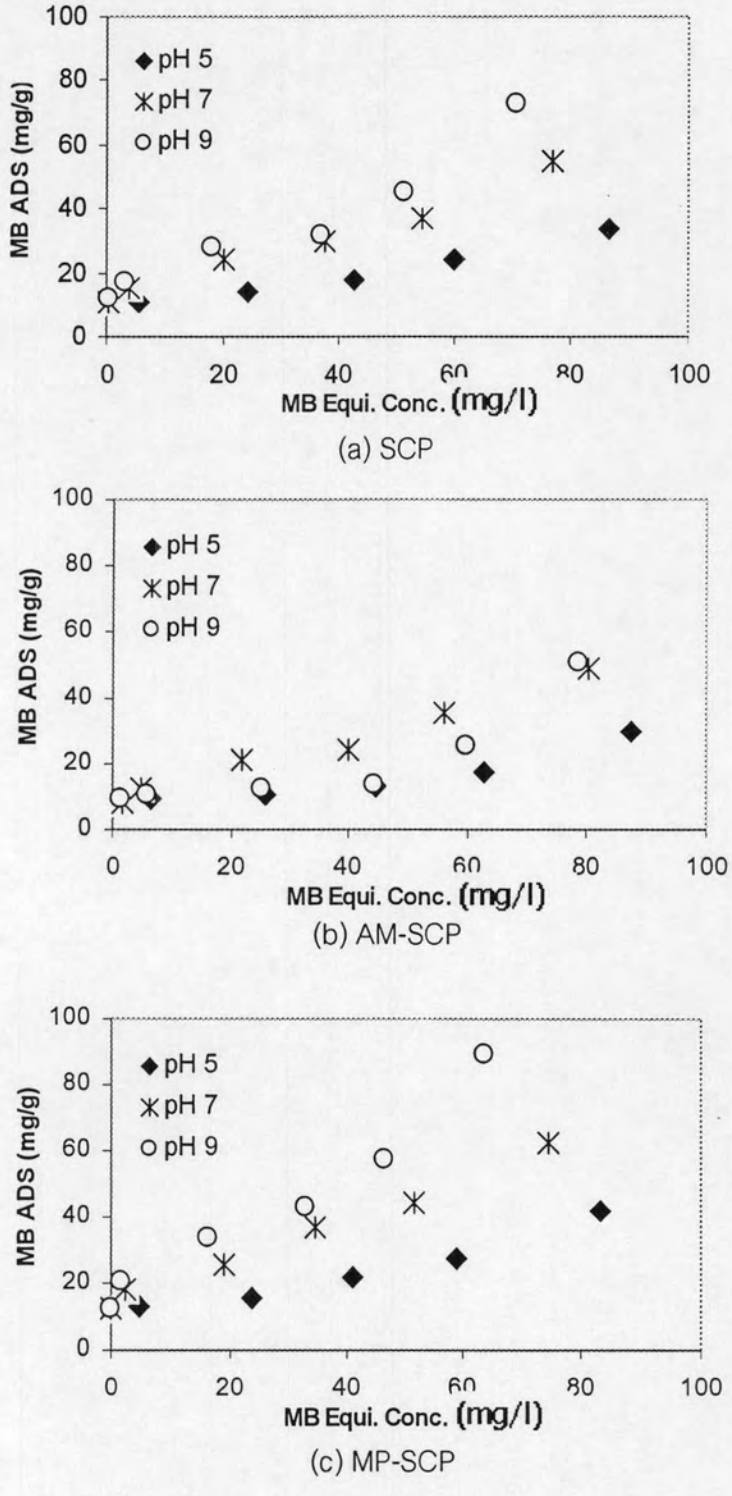

Figure 4.36 Adsorption isotherm of MB adsorption onto (a) SCP, (b) AM-SCP and (c) MP-SCP at different pH, Temperature 25 °C and Ionic strength 0.01 M.

Table 4.16 Parameters of Langmuir and Freundlich isotherm model for Cu(II) adsorption on SCP, AM-SCP and MP-SCP at pH 3 and 5.

Adsorbent	Langmuir			Freundlich		
pH	q_m	K_L	R^2	K_f	n	R^2
SCP						
3	0.1764	2.9044	0.9780	0.9294	1.2694	0.9656
5	3.6928	0.3272	0.8736	2.3518	1.2736	0.9739
AM-SCP						
3	4.5725	0.3765	0.9984	3.1653	1.6098	0.9888
5	4.7081	3.7929	0.5755	0.6553	1.9685	0.8248
MP-SCP						
3	21.2314	0.2324	0.7240	0.5786	2.0354	0.9256
5	6.2267	5.4074	0.6346	0.3528	1.9940	0.8767

Table 4.17 Parameters of Langmuir and Freundlich isotherm model for Pb(II) adsorption on SCP, AM-SCP and MP-SCP at pH 3 and 5.

Adsorbent	Langmuir			Freundlich		
pH	q_m	K_L	R^2	K_f	n	R^2
SCP						
3	0.7479	0.7314	0.8165	0.5551	1.7227	0.9338
5	3.2541	0.4053	0.9528	2.4316	1.4691	0.9734
AM-SCP						
3	1.8847	0.7104	0.8627	1.7071	1.6351	0.9449
5	6.5746	0.2382	0.9810	2.7504	1.4966	0.9746
MP-SCP						
3	2.8588	0.5981	0.8516	3.2065	1.4497	0.9581
5	4.9407	0.4686	0.9902	2.0047	1.6545	0.9906

Table 4.18 Parameters of Langmuir and Freundlich isotherm model for Cd(II) adsorption on SCP, AM-SCP and MP-SCP at pH 3 and 5.

Adsorbent	Langmuir			Freundlich		
pH	q_m	K_L	R^2	K_f	n	R^2
SCP						
3	7.3206	0.0372	0.9985	0.5339	1.0819	0.9861
5	8.5106	0.1388	0.9707	1.5292	1.1480	0.9758
AM-SCP						
3	1.2809	0.1249	0.8962	0.4249	0.9237	0.9384
5	8.5106	0.1388	0.9975	4.2064	1.2282	0.9945
MP-SCP						
3	2.9214	0.4818	0.9681	2.4430	1.5738	0.9721
5	4.3573	1.0470	0.8948	1.3295	1.8175	0.9602

Table 4.19 Parameters of Langmuir and Freundlich isotherm model for acid blue 45 (AB) adsorption on SCP, AM-SCP and MP-SCP at pH 5, 7 and 9.

Adsorbent	Langmuir			Freundlich		
pH	q_m	K_L	R^2	K_f	n	R^2
SCP						
5	22.2717	0.1930	0.9967	0.2356	3.3557	0.9258
7	17.3611	0.2110	0.9293	0.4099	3.0497	0.9894
9	8.3056	0.2173	0.9422	0.8430	3.7425	0.9869
AM-SCP						
5	39.8406	6.2750	0.8440	0.3067	5.3022	0.9763
7	36.2319	3.7808	0.7871	0.2536	4.8852	0.9603
9	19.2678	0.3318	0.9964	0.1292	4.4803	0.9435
MP-SCP						
5	17.6056	0.0500	0.9134	0.5829	3.4722	0.9767
7	9.9108	0.2194	0.9464	0.6888	3.6968	0.9781
9	11.4155	0.1752	0.9894	0.6864	3.3580	0.9818

Table 4.20 Parameters of Langmuir and Freundlich isotherm model for methylene blue (MB) adsorption on SCP, AM-SCP and MP-SCP at pH 5, 7 and 9.

Adsorbent	Langmuir			Freundlich		
pH	q_m	K_L	R^2	K_f	n	R^2
SCP						
5	17.8891	2.7811	0.3842	0.0005	5.1653	0.6907
7	28.7356	1.6571	0.7405	0.0957	3.6778	0.9029
9	32.6797	2.5714	0.7280	0.1698	3.6832	0.8560
AM-SCP						
5	14.4718	0.8758	0.4110	0.2081	4.1237	0.6486
7	32.3625	0.1657	0.9505	0.2586	2.2738	0.9608
9	17.6056	0.8516	0.4168	0.1666	3.3434	0.5652
MP-SCP						
5	20.4499	6.1125	0.3922	0.0948	5.6948	0.6465
7	31.9488	8.6944	0.7107	0.2348	4.7755	0.8607
9	39.5257	6.1707	0.7841	0.2792	3.9216	0.8907

4.3.3 Adsorption isotherm of bi solute

4.3.3.1 Cu(II) and Acid blue

Figure 4.37-4.42 illustrated adsorption isotherms in bi-solute between Cu(II) and AB. Effect of Cu(II) on AB adsorption capacity was studied by varying concentration of Cu(II) from 0 to 10 mg/l and fixed concentration of AB at 50 mg/l, which were studies by mixing solution. In addition, effect of AB on Cu(II) adsorption capacity was studied by varying concentration of AB from 0 to 100 mg/l and fixed concentration of Cu(II) at 5 mg/l, which were studies by mixing solution.

To study the effect of coexisting compound, the adsorption isotherms in bi-solute were compared with adsorption isotherms in single-solute. The results showed that the presence of Cu(II) didn't affect to adsorption capacity AB directly for all adsorbents because of low surface competition of Cu(II) and AB. This might be explained that amount of adsorbed Cu(II) and AB was not equivalent to the functional groups on the surfaces, hence, the active site was still remained for the other pollutants to be adsorbed on the same surface.

The adsorption isotherm of Cu(II) on SCP has slightly decreased when AB exists in the bi-solution. Moreover, the adsorption isotherms showed that the adsorption capacity of AB on SCP has not changed when Cu(II) existed in the bi-solution, comparing with the single solution isotherm. The amount of Cu(II) and AB adsorption capacities are staying still at around 3 and 10 mg/g, respectively. These results showed that the existence of both Cu(II) and AB are not effected to the adsorption capacity on SCP surface each other, significantly.

The adsorption isotherm showed that the adsorption capacity of AB on MP-SCP has not changed significantly when Cu(II) included in the bi-solution which comparing with the single solution isotherm. The amount of Cu(II) and AB adsorption capacities are staying still at around 10 and 20 mg/g for Cu(II) and AB respectively.

The adsorption isotherm of Cu(II) and AB in bi solute on AM-SCP showed that the adsorption capacity had no change significantly in the bi-solution, comparing with the single solution isotherm. The amount of Cu(II) and AB adsorption capacities are staying still at around 5.5 and 46 mg/g, respectively.

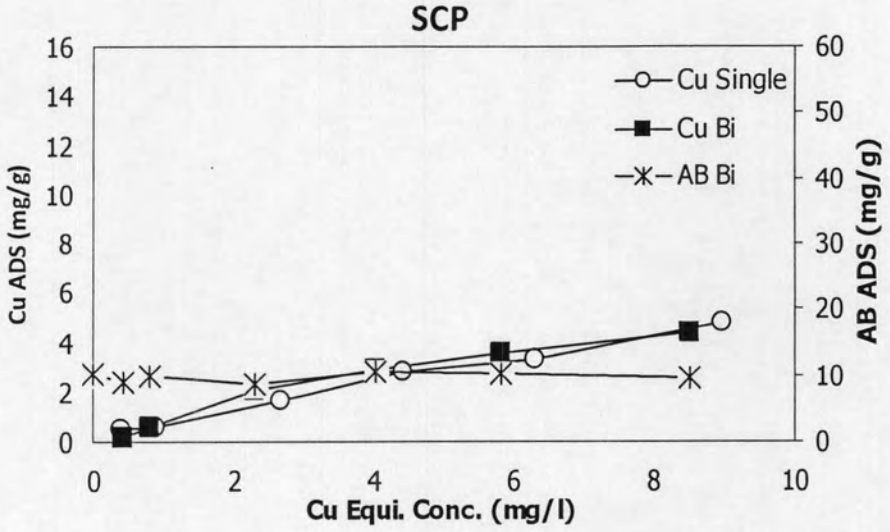

Figure 4.37 Adsorption capacity of Cu(II) onto SCP by fixing initial AB concentration under mixing with various Cu(II) concentration at pH 5, Temperature 25 °C and Ionic strength 0.01 M.

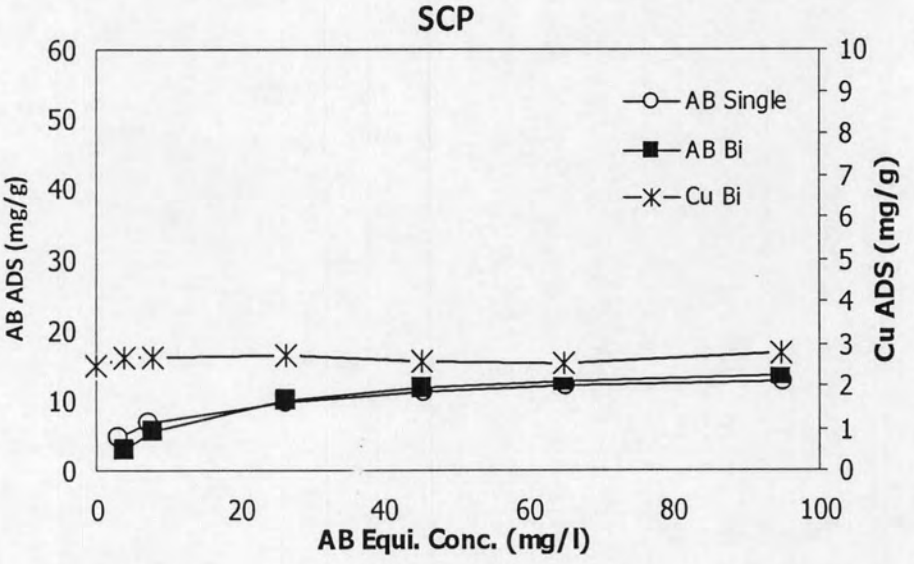

Figure 4.38 Adsorption capacity of AB onto SCP by fixing initial Cu(II) concentration under mixing with various AB concentration at pH 5, Temperature 25 °C and Ionic strength 0.01 M.

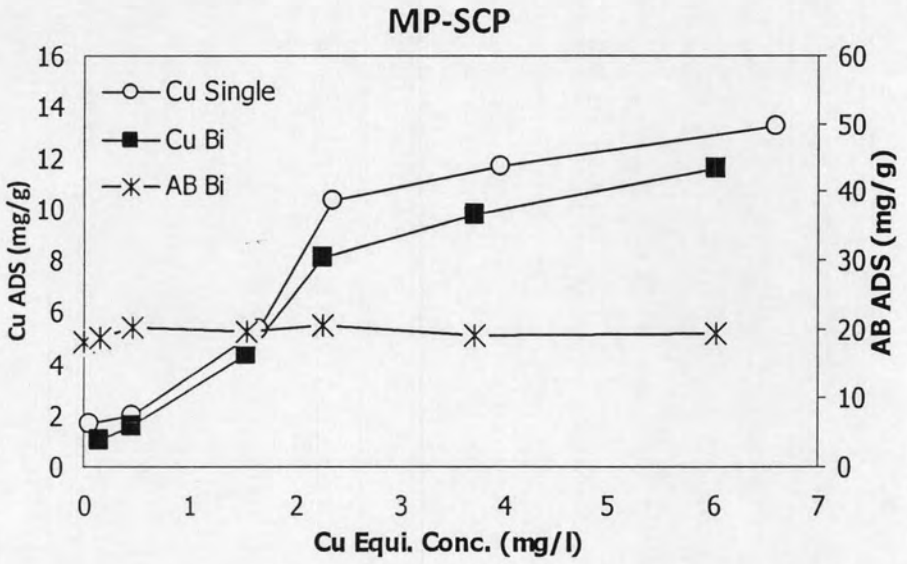

Figure 4.39 Adsorption capacity of Cu(II) onto MP-SCP by fixing initial AB concentration under mixing with various Cu(II) concentration at pH 5, Temperature 25 °C and Ionic strength 0.01 M.

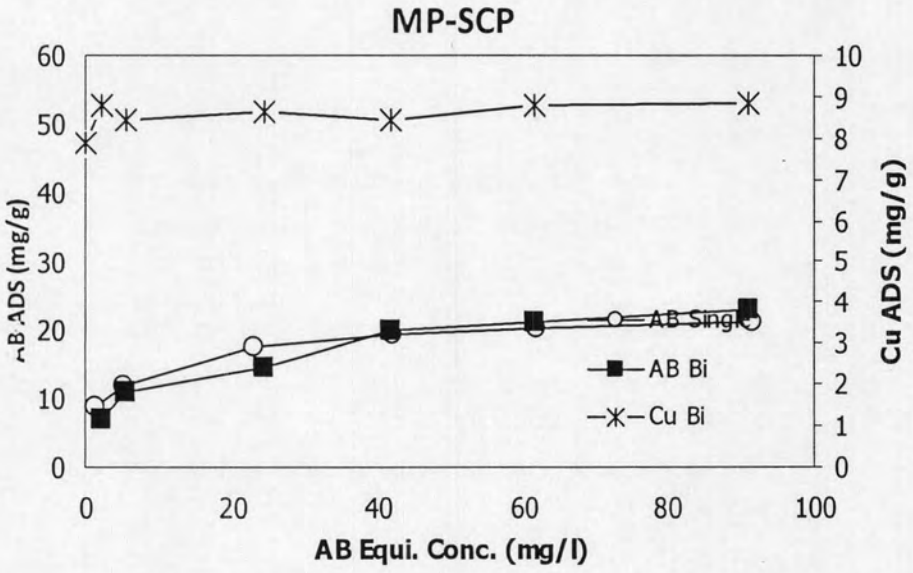

Figure 4.40 Adsorption capacity of AB onto MP-SCP by fixing initial Cu(II) concentration under mixing with various AB concentration at pH 5, Temperature 25 °C and Ionic strength 0.01 M.

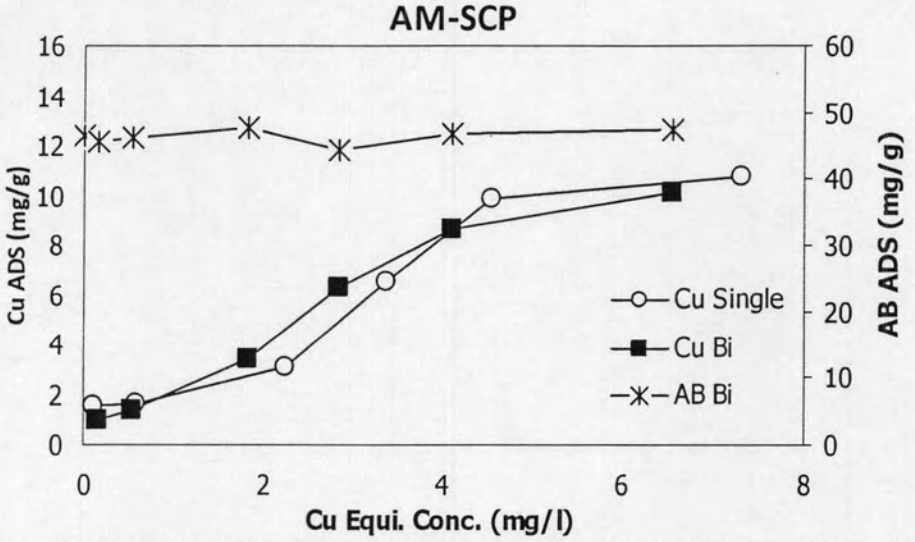

Figure 4.41 Adsorption capacity of Cu(II) onto AM-SCP by fixing initial AB concentration under mixing with various Cu(II) concentration at pH 5, Temperature 25 °C and Ionic strength 0.01 M.

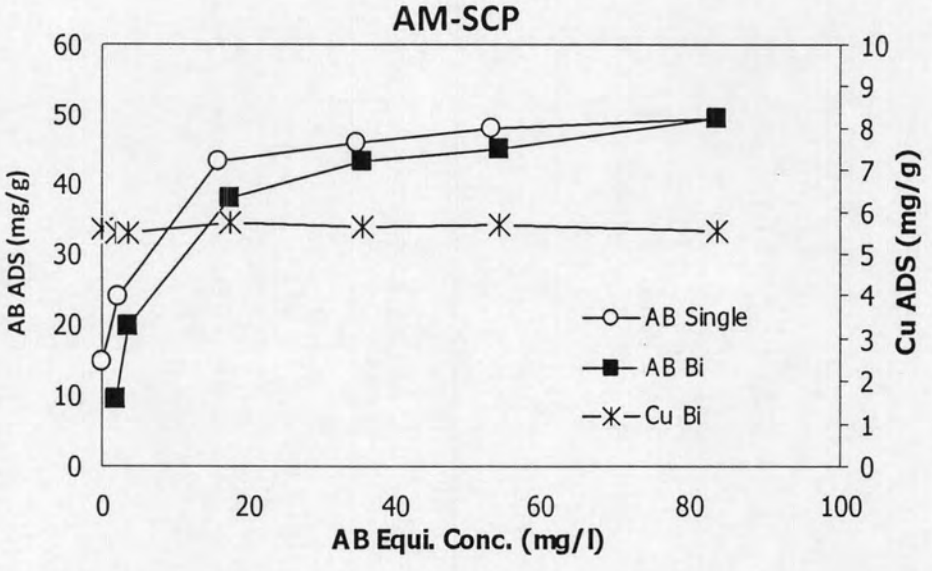

Figure 4.42 Adsorption capacity of AB onto AM-SCP by fixing initial Cu(II) concentration under mixing with various AB concentration at pH 5, Temperature 25 °C and Ionic strength 0.01 M.

4.3.3.2 Cu(II) and Methylene blue

Figure 4.43 - 4.48 illustrated adsorption isotherms in binary solute between Cu(II) and MB. Effect of Cu(II) on MB adsorption capacity was studied by varying concentration of Cu(II) from 0 to 10 mg/l and fixed concentration of MB at 50 mg/l, which were studies by mixing solution. In addition, effect of MB on Cu(II) adsorption capacity was studied by varying concentration of MB from 0 to 100 mg/l and fixed concentration of Cu(II) at 5 mg/l, which were studies by mixing solution.

To study the effect of coexisting compound, the adsorption isotherms in bi-solute were compared with adsorption isotherms in single-solute. The results showed that the presence of Cu(II) didn't affect to adsorption capacity MB directly for AM-SCP and MP-SCP, except for SCP, since low surface competition of Cu(II) and AB. This might be explained that amount of adsorbed Cu(II) and AB was not equivalent to the functional groups on the surfaces, hence, the active site was still remained for the other pollutants to be adsorbed on the same surface. Adsorption of MB on the SCP surface trend to be increase when Cu(II) was added in the solution, that might be caused by the MB can be also interact with the functional group which adsorbed Cu(II) on the SCP surface.

The adsorption isotherm of Cu(II) on SCP has slightly increased when MB exists in the bi-solution. Moreover, the adsorption isotherms showed that the adsorption capacity of MB on SCP has not changed when Cu(II) existed in the bi-solution, comparing with the single solution isotherm. The amount of Cu(II) and MB adsorption capacities are around 12 and 1.5 mg/g, respectively. The adsorption isotherm showed that the adsorption capacity of MB on MP-SCP has not changed significantly when Cu(II) included in the bi-solution which comparing with the single solution isotherm. The amount of Cu(II) and MB adsorption capacities are staying still at around 8.5 and 16 mg/g for Cu(II) and AB respectively.

The adsorption isotherm of Cu(II) and MB in bi solute on AM-SCP showed that the adsorption capacity had no change significantly in the bi-solution, comparing with the single solution isotherm. The amount of Cu(II) and MB adsorption capacities are staying still at around 5.2 and 12 mg/g, respectively.

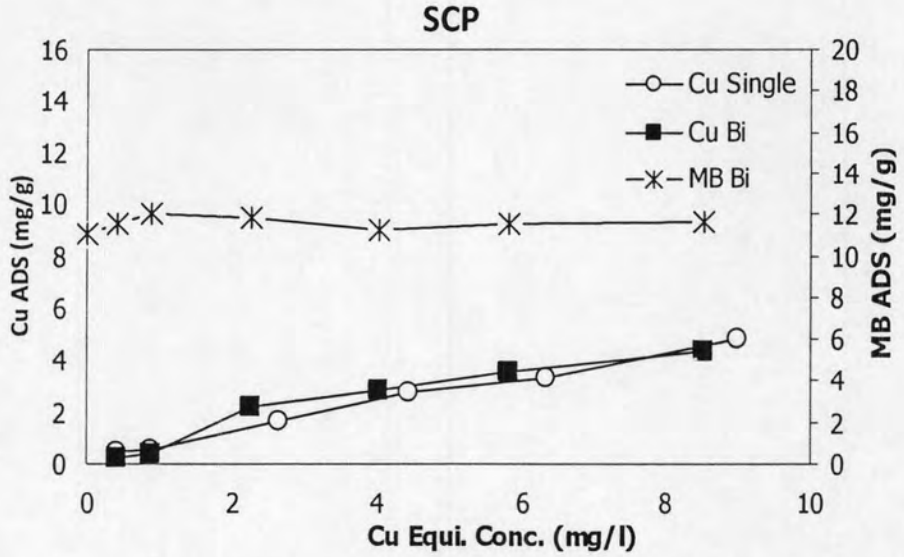

Figure 4.43 Adsorption capacity of Cu(II) onto SCP by fixing initial MB concentration under mixing with various Cu(II) concentration at pH 5, Temperature 25 °C and Ionic strength 0.01 M.

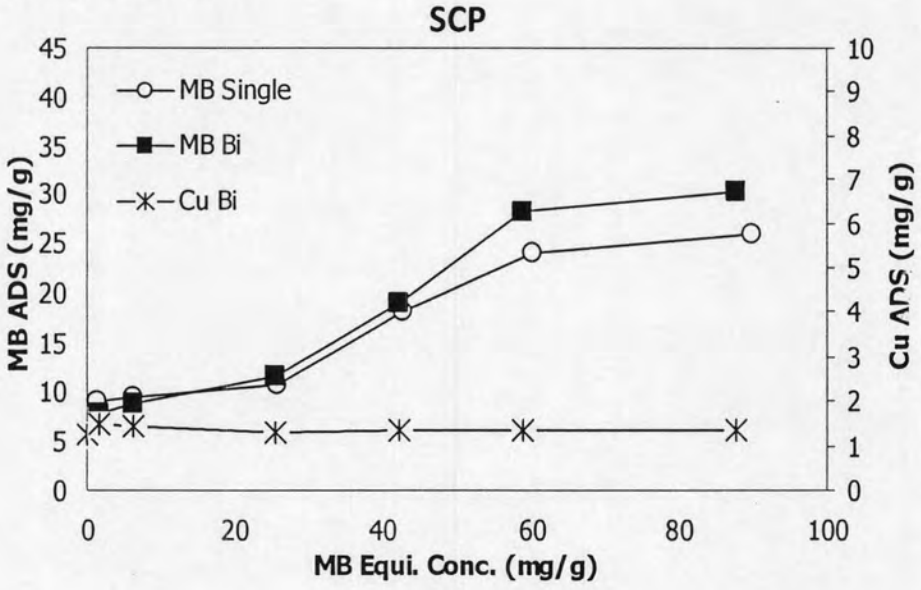

Figure 4.44 Adsorption capacity of MB onto SCP by fixing initial Cu(II) concentration under mixing with various MB concentration at pH 5, Temperature 25 °C and Ionic strength 0.01 M.

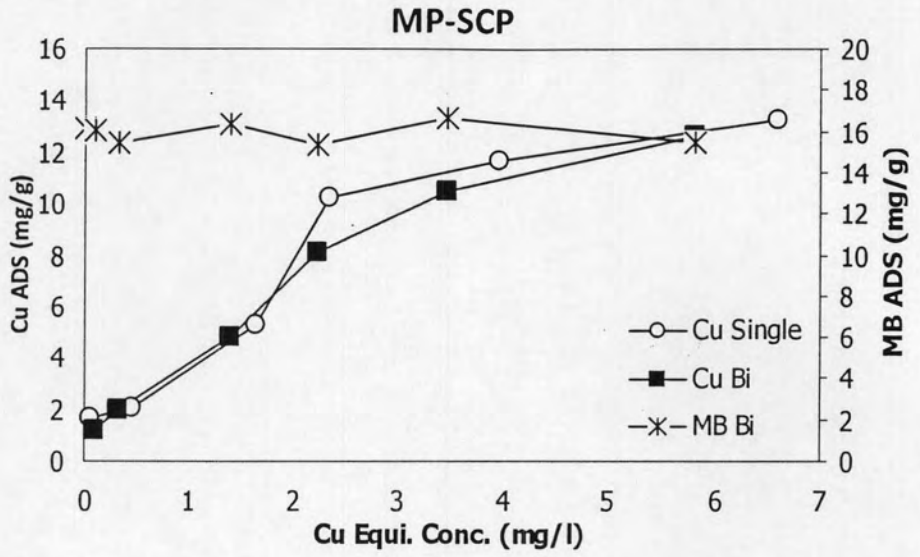

Figure 4.45 Adsorption capacity of Cu(II) onto MP-SCP by fixing initial MB concentration under mixing with various Cu(II) concentration at pH 5, Temperature 25 °C and Ionic strength 0.01 M.

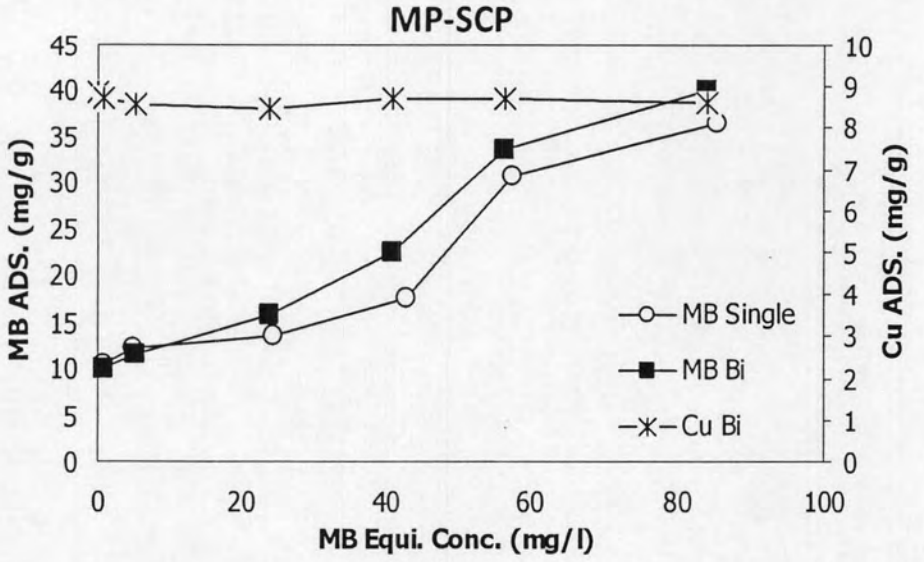

Figure 4.46 Adsorption capacity of MB onto MP-SCP by fixing initial Cu(II) concentration under mixing with various MB concentration at pH 5, Temperature 25 °C and Ionic strength 0.01 M.

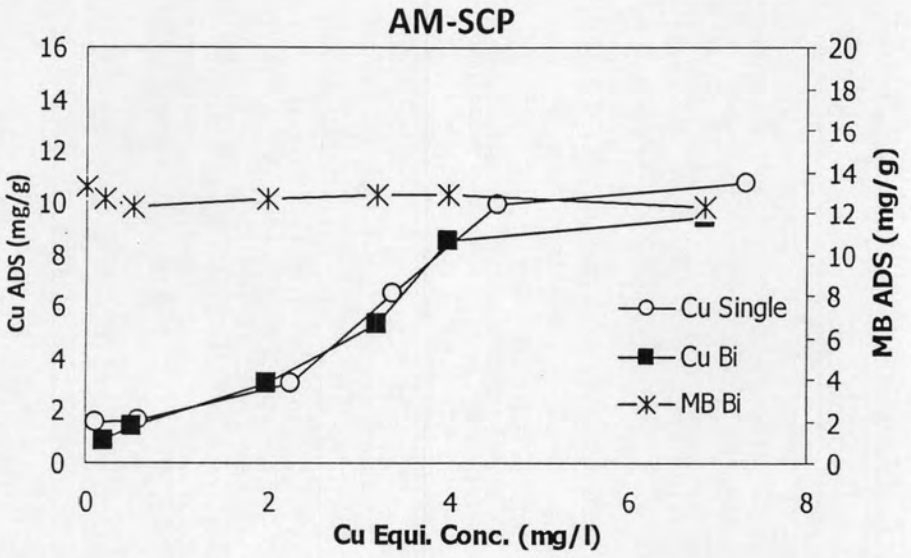

Figure 4.47 Adsorption capacity of Cu(II) onto AM-SCP by fixing initial MB concentration under mixing with various Cu(II) concentration at pH 5, Temperature 25 °C and Ionic strength 0.01 M.

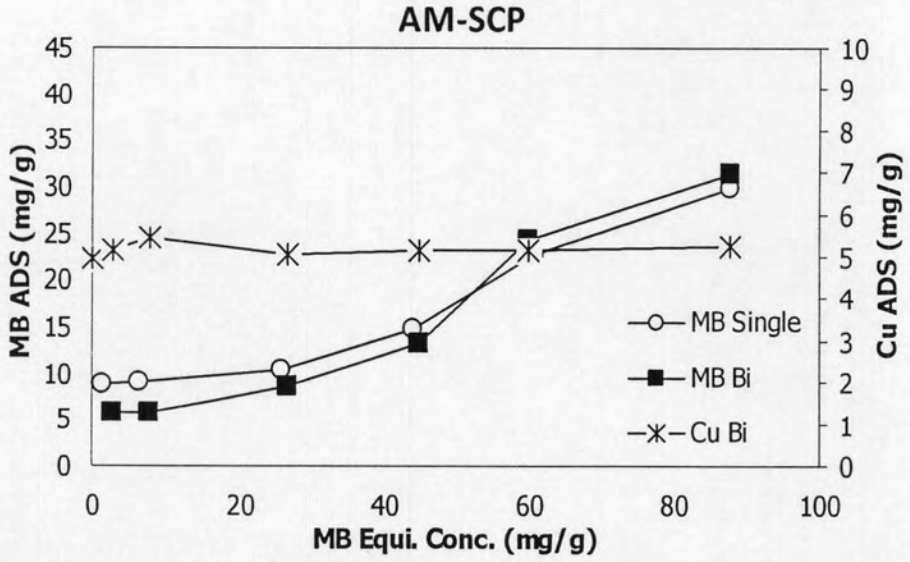

Figure 4.48 Adsorption capacity of MB onto AM-SCP by fixing initial Cu(II) concentration under mixing with various MB concentration at pH 5, Temperature 25 °C and Ionic strength 0.01 M.

4.4 Separation

Separation for SCP and functionalized SCPs were performed by varying amount of adsorbent and pH, including with the existing of pollutants. Separation by magnet efficiency was measured by turbidity meter. We compared the remove silica nanoparticles results to those obtained by Ching-Ju et al (2006) studied magnetite nanoparticles were synthesized as magnetic seeding particles to remove silica nanoparticles from chemical mechanical polishing wastewaters by magnetic seeding aggregation, which was achieved by electrostatic attractions for they are highly oppositely charged. When the seeded wastewater was placed in a magnetic field higher than 800 G, the turbidity of the wastewater was reduced to 1 NTU.

4.4.1 Effect of pH to separation efficiency

Lorentz force is the force on a point charge due to electromagnetic fields. It is given by the following equation in terms of the electric and magnetic fields. A positively charged particle will be accelerated in the same linear orientation as the E field, but will curve perpendicularly to both the instantaneous velocity vector v and the B field according to the right-hand rule (in detail, if the thumb of the right hand points along v and the index finger along B, then the middle finger points along F). The term qE is called the electric force, while the term qv × B is called the magnetic force.[3] According to some definitions, the term Lorentz force refers specifically to the formula for the magnetic force (Griffiths, 1999).

$$\mathbf{F}_{mag} = q(\mathbf{v} \times \mathbf{B})$$

where

F is the force (newtons)

B is the magnetic field (teslas)

q is the electric charge of the particle (coulombs)

v is the instantaneous velocity of the particle (metres per second)

× is the vector cross product

If this empirical statement is valid (and, of course, countless experiments have shown that it is), then two vector fields E and B are thereby defined throughout space and time, and these are called the "electric field" and "magnetic field". Note that the fields are defined everywhere in space and time, regardless of whether or not a charge is present to experience the force. In particular, the fields are defined with respect to what force a test charge would feel, if it were hypothetically placed there. A definition of E and B, the Lorentz force is only a definition in principle because a real particle would generate its own finite E and B fields, which would alter the electromagnetic force that it experiences. In addition, if the charge experiences acceleration, for example, if forced into a curved trajectory by some external agency, it emits radiation that causes braking of its motion. These effects occur through both a direct effect (called the radiation reaction force) and indirectly (by affecting the motion of nearby charges and currents). Moreover, the electromagnetic force is not in general the same as the net force, due to gravity, electroweak and other forces, and any extra forces would have to be taken into account in a real measurement (Jackson, 1998).

Table 4.21 shows the effect of magnetic field on separation efficiency. It was clear that adding magnetic filed at 3500 gauss could enhance sedimentation efficiency of SCP at pH 2 from 82.5% to 99.5%. The effect of pH on the separation efficiency on SCP, AM-SCP and MP-SCP from water were evaluated within the range of 2 to 12. At pH 2, the separation efficiency SCP, AM-SCP and MP-SCP (99.11%, 99.72%and 99.62%, respectively) higher than at other pH that showed in Table 4.22-4.24. The magnet was decrease the turbidity of SCP, AM-SCP and MP-SCP from water about 850 to 5 NTU. The hydrophobicity on MP-SCP did not increase the separation efficiency, significant. However, separation efficiencies of MP-SCP at every pH were slightly higher than SCP. At low pH around 2, the surface charge of the particles were protonated to be positive which supposed that can decrease the sedimentation efficiency of particles or colloid in the water due to the repulsive force. But the obtained results exhibit the highest removal efficiencies for all particles. Hence, the effect of positive charge intensity that can enhance the Lorentz force due to the added magnetic

filed. However, when the pH increased higher than pH_{zpc} , the surface charge of the particles trend to be negative, but it did not affect to separation efficiency of studied SCP significantly. It might be concluded the positive charge of particles can enhance the sedimentation of the particles by magnetic filed.

Table 4.21 Effect of magnetic field on separation efficiency of SCP at pH 2.

SCP: pH 2 (0.1g/100 ml)	Turbidity (NTU)	
Time (min)	3500 gauss	-
0	781	763
30	14.20	156
60	5.30	136
eff. %	99.32	82.5

Table 4.22 Separation efficiency of SCP 0.1g / 100 ml at different pH.

SCP (0.1g/100ml)	Turbidity (NTU)						
Time(min)	pH2	pH3	pH4	pH5	pH7	pH9	pH12
0	825.4	831.3	826.8	828.2	840.4	834.5	824.2
30	10.41	34.54	42.25	54.5	49.25	42.67	40.5
60	7.32	15.75	24.86	29.24	26.5	23.16	24.25
eff. %	99.11	98.11	96.99	96.47	96.85	97.22	97.06

Table 4.23 Separation efficiency of MP- SCP 0.1g / 100 ml at different pH.

MP-SCP (0.1g/100ml)	Turbidity (NTU)						
Time(min)	pH2	pH3	pH4	pH5	pH7	pH9	pH12
0	875.8	880.8	854.6	835.8	870.5	845.1	876.4
30	5.65	10.92	12.63	20.49	22.84	18.87	16.12
60	2.44	4.39	5.98	10.54	12.48	10.66	13.55
eff. %	99.72	99.50	99.30	98.74	98.57	98.74	98.45

Table 4.24 Separation efficiency of AM- SCP 0.1g / 100 ml. at different pH.

AM-SCP (0.1g/100ml)	Turbidity (NTU)						
Time(min)	pH2	pH3	pH4	pH5	pH7	pH9	pH12
0	861.3	869.7	883.2	865.4	868.5	874.3	879.1
30	10.55	15.16	23.45	36.23	40.34	32.68	28.49
60	6.36	8.48	10.44	21.3	24.75	22.03	18.52
eff. %	99.26	99.02	98.82	97.54	97.15	97.48	97.89

4.4.2 Effect on weight adsorbent to separation efficiency

The effect of weight of adsorbent on the separation efficiency on SCP, AM-SCP and MP-SCP from water were evaluated within the range of 0.05 to 0.6g per 100 ml. The separation efficiencies on 0.05g of SCP, AM-SCP and MP-SCP were higher than the other (99.24%, 99.75%and 99.41%, respectively) that showed in Table 4.25-4.27. However, removal efficiency of all particles still remained over 99% until 0.01 g per 100ml. Moreover, increasing of amount of particle might increase the repulsive force of the same negative charge particle, result to the lower sedimentation efficiency.

Table 4.25 Separation efficiency of SCP at pH 2 with different weight.

pH 2	Weight SCP (g)				
	Turbidity(NTU)				
Time	0.05	0.1	0.2	0.4	0.6
0	444.5	845.4	1302	1960	3524
30	10.29	16.1	20.55	59.14	67.77
60	3.39	7.39	13.61	28.55	46.48
eff. %	99.24	99.13	98.96	98.54	98.68

Table 4.26 Separation efficiency of MP-SCP at pH 2 with different weight.

pH 2	Weight MP-SCP (g)				
	Turbidity(NTU)				
Time	0.05	0.1	0.2	0.4	0.6
0	441.3	854.7	1406	2247	3416
30	3.86	5.76	12.67	32.34	46.84
60	1.12	2.35	6.77	14.18	18.9
eff. %	99.75	99.73	99.52	99.37	99.45

Table 4.27 Separation efficiency of AM-SCP at pH 2 with different weight.

pH 2	Weight AM-SCP (g)				
	Turbidity(NTU)				
time	0.05	0.1	0.2	0.4	0.6
0	474.4	870.8	1375	2084	3641
30	5.65	9.65	20.34	54.29	70.62
60	2.82	5.28	14.16	27.55	38.46
eff. %	99.41	99.39	98.97	98.68	98.94

4.4.3 Effect of the presence of pollutants (Cu(II), AB and MB) to separation efficiency

Table 4.28-4.30 show the effect of the existence of Cd(II) on removal efficiencies of SCP, AM-SCP and MP-SCP. It was found that the adsorption of Cd(II) on the surfaces did not affected to the sedimentation efficiency of SCP, AM-SCP and MP-SCP particles from synthetic wastewater. Separation efficiencies of Cd(II) adsorbed particles, higher than 98%, were not different form non-adsorption particles, by comparing efficiency in particle separation in different concentration of Cd(II), 1 and 10 mg/L on SCP (99.17% and 98.88% respectively), AM-SCP (99.69% and 99.61% respectively) and MP-SCP (99.74% and 99.80% respectively). In addition, the efficiency in particle separation in different weight of adsorbent was not different significantly.

Table 4.28 Separation efficiency of SCP at pH 2 with the presence of Cd(II).

SCP: pH2	Turbidity(NTU)			
	SCP 0.05 g / 100 ml		SCP 0.1 g / 100 ml	
	Concentration of Cd(II) (mg/L)			
time	1	10	1	10
0	453.00	448.25	842.90	843.15
30	12.21	15.06	21.29	23.23
60	3.77	5.03	5.09	6.50
eff. %	99.17	98.88	99.40	99.23

Table 4.29 Separation efficiency of AM-SCP at pH 2 with the presence of Cd(II).

AM-SCP: pH2	Turbidity(NTU)			
	AM-SCP 0.05 g / 100 ml		AM-SCP 0.1 g / 100 ml	
	Concentration of Cd(II) (mg/L)			
time	1	10	1	10
0	476.40	481.75	866.70	890.15
30	6.31	7.16	8.62	9.28
60	1.48	1.89	2.44	3.16
eff. %	99.69	99.61	99.72	99.65

Table 4.30 Separation efficiency of MP-SCP at pH 2 with the presence of Cd(II).

MP-SCP: pH2	Turbidity(NTU)			
	MP-SCP 0.05 g / 100 ml		MP-SCP 0.1 g / 100 ml	
	Concentration of Cd(II) (mg/L)			
Time	1	10	1	10
0	430.65	460.60	834.35	868.85
30	3.35	3.44	4.16	4.56
60	1.10	0.93	1.56	1.74
eff. %	99.74	99.80	99.81	99.80

Table 4.31-4.33 show the effect of the existence of Cu(II) on removal efficiencies of SCP, AM-SCP and MP-SCP. It was found that the adsorption of Cu(II) on the surfaces did not affected to the sedimentation efficiency of SCP, AM-SCP and MP-SCP particles from synthetic wastewater. Separation efficiencies of Cu(II) adsorbed particles, higher than 99%, were not different form non-adsorption particles, by comparing efficiency in particle separation in different concentration of Cu(II), 1 and 10 mg/L on SCP (99.32% and 99.24% respectively), (99.28% and 99.25% respectively) and MP-SCP (99.81% and 99.81% respectively). In addition, the efficiency of particle separation in different weight of adsorbent was not different significantly.

Table 4.31 Separation efficiency of SCP at pH 2 with the presence of Cu(II).

SCP: pH2	Turbidity(NTU)			
	SCP 0.05 g / 100 ml		SCP 0.1 g / 100 ml	
	Concentration of Cu(II) (mg/L)			
Time	1	10	1	10
0	451.70	459.40	858.75	869.00
30	7.93	8.57	8.92	10.33
60	3.09	3.48	4.84	5.24
eff. %	99.32	99.24	99.44	99.40

Table 4.32 Separation efficiency of AM-SCP at pH 2 with the presence of Cu(II).

AM-SCP: pH2	Turbidity(NTU)			
	AM-SCP 0.05 g / 100 ml		AM-SCP 0.1 g / 100 ml	
	Concentration of Cu(II) (mg/L)			
time	1	10	1	10
0	471.10	474.00	861.55	873.00
30	7.82	8.33	9.20	8.33
60	3.40	3.54	4.42	5.20
eff. %	99.28	99.25	99.49	99.40

Table 4.33 Separation efficiency of MP-SCP at pH 2 with the presence of Cu(II).

MP-SCP: pH2	Turbidity(NTU)			
	MP-SCP 0.05 g / 100 ml		MP-SCP 0.1 g / 100 ml	
	Concentration of Cu(II) (mg/L)			
time	1	10	1	10
0	483.55	496.05	884.35	877.35
30	4.13	4.23	5.47	5.17
60	0.90	0.95	1.54	1.63
eff. %	99.81	99.81	99.83	99.81

Table 4.34-4.36 show the effect of the existence of Pb(II) on removal efficiencies of SCP, AM-SCP and MP-SCP. It was found that the adsorption of Pb(II) on the surfaces did not affected to the sedimentation efficiency of SCP, AM-SCP and MP-SCP particles from synthetic wastewater. Separation efficiencies of Pb(II) adsorbed particles, higher than 99%, were not different form non-adsorption particles, by comparing efficiency in particle separation in different concentration of Pb(II), 1 and 10 mg/L on SCP (99.18% and 99.14% respectively), AM-SCP (99.15% and 99.03% respectively) and MP-SCP (99.72% and 99.68% respectively). In addition, the efficiency of particle separation in different weight of adsorbent was not different significantly.

Table 4.34 Separation efficiency of SCP at pH 2 with the presence of Pb(II).

SCP: pH2	Turbidity(NTU)			
	SCP 0.05 g / 100 ml		SCP 0.1 g / 100 ml	
	Concentration of Pb(II) (mg/L)			
Time	1	10	1	10
0	439.60	442.05	837.40	848.90
30	11.71	12.85	13.24	13.60
60	3.61	3.82	5.39	4.67
eff. %	99.18	99.14	99.36	99.45

Table 4.35 Separation efficiency of AM-SCP at pH 2 with the presence of Pb(II).

AM-SCP: pH2	Turbidity(NTU)			
	AM-SCP 0.05 g / 100 ml		AM-SCP 0.1 g / 100 ml	
	Concentration of Pb(II) (mg/L)			
Time	1	10	1	10
0	457.75	460.90	867.30	860.90
30	9.62	10.98	11.12	12.42
60	3.87	4.48	5.34	5.53
eff. %	99.15	99.03	99.38	99.36

Table 4.36 Separation efficiency of MP-SCP at pH 2 with the presence of Pb(II).

MP-SCP: pH2	Turbidity(NTU)			
	MP-SCP 0.05 g / 100 ml		MP-SCP 0.05 g / 100 ml	
	Concentration of Pb(II) (mg/L)			
time	1	10	1	10
0	462.05	475.40	877.80	881.65
30	3.83	4.20	6.75	4.20
60	1.29	1.53	2.18	1.53
eff. %	99.72	99.68	99.75	99.83

Table 4.37-4.39 show the effect of the existence of AB on removal efficiencies of SCP, AM-SCP and MP-SCP. It was found that the adsorption of AB on the surfaces did not affected to the sedimentation efficiency of SCP, AM-SCP and MP-SCP particles from synthetic wastewater. Separation efficiencies of AB adsorbed particles, higher than 98%, were not different form non-adsorption particles, by comparing efficiency in particle separation, 0 and 100 mg/L on SCP (99.24% and 98.89% respectively), AM-SCP (99.41% and 99.30% respectively) and MP-SCP (99.75% and 99.75% respectively). In addition, the efficiency of particle separation in different weight of adsorbent was not different significantly.

Table 4.37 Separation efficiency of SCP at pH 2 with the presence of AB.

SCP: pH2	Turbidity(NTU)			
	SCP 0.05 g / 100 ml		SCP 0.1 g / 100 ml	
	Concentration of AB (mg/L)			
Time	0	100	0	100
0	444.50	413.10	845.40	827.00
30	10.29	11.31	16.10	12.71
60	3.39	4.58	7.39	6.71
eff. %	99.24	98.89	99.13	99.19

Table 4.38 Separation efficiency of AM-SCP at pH 2 with the presence of AB.

AM-SCP: pH2	Turbidity(NTU)			
	AM-SCP 0.05 g / 100 ml		AM-SCP 0.1 g / 100 ml	
	Concentration of AB (mg/L)			
time	0	100	0	100
0	474.40	467.55	870.80	867.55
30	5.65	12.92	9.65	14.23
60	2.82	3.29	5.28	4.31
eff. %	99.41	99.30	99.39	99.50

Table 4.39 Separation efficiency of MP-SCP at pH 2 with the presence of AB.

MP-SCP: pH2	Turbidity(NTU)			
	MP-SCP 0.05 g / 100 ml		MP-SCP 0.1 g / 100 ml	
	Concentration of AB (mg/L)			
Time	0	100	0	100
0	441.30	505.00	854.70	866.05
30	3.86	14.50	5.76	15.17
60	1.12	1.28	2.35	1.67
eff. %	99.75	99.75	99.73	99.81

Table 4.40-4.42 show the effect of the existence of MB on removal efficiencies of SCP, AM-SCP and MP-SCP. It was found that the adsorption of MB on the surfaces did not affected to the sedimentation efficiency of SCP, AM-SCP and MP-SCP particles from synthetic wastewater. Separation efficiencies of MB adsorbed particles, higher than 98%, were not different form non-adsorption particles, by comparing efficiency in particle separation, 0 and 100 mg/L on SCP (99.24% and 98.95% respectively), AM-SCP (99.41% and 99.07% respectively) and MP-SCP (99.75% and 99.61% respectively). In addition, the efficiency of particle separation in different weight of adsorbent was not different significantly.

Table 4.40 Separation efficiency of SCP at pH 2 with the presence of MB.

SCP: pH2	Turbidity(NTU)			
	SCP 0.05 g / 100 ml		SCP 0.1 g / 100 ml	
	Concentration of MB (mg/L)			
time	0	100	0	100
0	444.50	438.95	845.40	855.05
30	10.29	12.29	16.10	13.25
60	3.39	4.63	7.39	6.64
eff. %	99.24	98.95	99.13	99.22

Table 4.41 Separation efficiency of AM-SCP at pH 2 with the presence of MB.

AM-SCP: pH2	Turbidity(NTU)			
	AM-SCP 0.05 g / 100 ml		AM-SCP 0.1 g / 100 ml	
	Concentration of MB (mg/L)			
Time	0	100	0	100
0	474.40	458.35	870.80	862.05
30	5.65	14.09	9.65	17.55
60	2.82	4.28	5.28	5.66
eff. %	99.41	99.07	99.39	99.34

Table 4.42 Separation efficiency of MP-SCP at pH 2 with the presence of MB.

MP-SCP: pH2	Turbidity(NTU)			
	MP-SCP 0.05 g / 100 ml		MP-SCP 0.1 g / 100 ml	
	Concentration of MB (mg/L)			
Time	0	100	0	100
0	441.30	479.95	854.70	885.20
30	3.86	13.39	5.76	17.04
60	1.12	1.88	2.35	2.18
eff. %	99.75	99.61	99.73	99.75